AS5213 Design of UAVs and MAVs
Technical Report

Medical delivery VTOL aircraft for defence applications

Submitted by:

Group Ravens
AE19B001 BAPU GAYATHRI MADDISETTY
AE19B011 SAI SAANDEEP. S
AE19B024 ADITYA VIJAY DHOBLE
AE19B027 ANDREA ELIZABETH BIJU
AE19B047 PURAM NIHAL
AE19B103 DRISHTI DARSHAN

Department of Aerospace Engineering
Indian Institute of Technology Madras

Contents

List of Figures

Acknowledgement

We like to express our gratitude to the Course Instructors, Prof. M. Ramakrishna and Prof. Bharath Govindarajan for their teaching and continuous support. They have been patient in clarifying our doubts and directing us towards the right path by asking us thought provoking questions. We would also like to thank our TA, Satya Kumar for his valuable feedback and suggestions.

Chapter 1

Mission Definition and Requirements

1.1 Mission Statement

The primary design objective is to "**design a Vertical Take-Off and Landing (VTOL) UAV that can be used to deliver emergency life-saving medical supplies like blood etc., specifically to defence areas**".

1.2 Necessity and Uniqueness of proposed Solution

We wish to design a delivery drone capable of delivering sensitive medical supplies and equipment faster and safer to the point of need, specifically designed to cater to the needs of the Indian military. This drone is designed to fly at high altitudes and under adverse conditions, unlike conventional delivery drones [1], [2]. Also, since medical supplies and equipment have to be delivered, several safety measures have to be incorporated into the design, while ensuring the ease of use as well as reliability [3]. All of these aspects make our proposed solution a unique one.

1.3 Inspiration

India's terrain is one of the most unique with very high irregularity. We have Siachen at an altitude of 5000m. Siachen stands to be the highest battlefield in the world with extremely low oxygen levels and very cold weather. The Indo-Pakistan border has blistering heat, sky high temperatures with frequent dust storms. Due to these volatile weather conditions there is a need to send medical supplies to the Armed forces remotely with as little human

presence required as possible [4]. This calls for the need of our mission. Our Vertical Take-Off and Landing (VTOL aircraft) UAV can be used to deliver emergency life-saving medical supplies in the toughest of terrains with control done remotely so that the purpose can be served without actual on the ground presence of humans. Our UAV doesn't need to land as the terrains can be very irregular, instead it will hover drop the packages wherever required.

1.4 Mission Requirements

This VTOL aircraft is supposed to supply medical equipment to armed force personnel in a remote area. The VTOL aircraft must consist of following characteristics to accomplish the task:

1. *Safe delivery of payload (medical equipment) within stipulated time.* Medical equipment which includes blood bags, saline bottles, antiseptic vials etc, which are delicate, are required to be safely transported by the VTOL aircraft. Throughout the mission, the payload must not be affected by any external stimuli such as sudden shifts and vibrations. The payload bay is to be designed to ensure safety and prevent any contamination of the equipment. The payload bay would also be equipped with a cooling facility to transport temperature sensitive payloads.
2. *Operable in extreme weather conditions.* As these VTOL aircrafts are to be utilised by the military forces, the target area could be remote in most cases. The Indian army is stationed at various locations with a vast range of climatic conditions from deserts to the Himalayas. The VTOL aircraft must be capable of safely maneuvering in presence of strong winds, at high altitudes or drastic temperature differences.
3. *Recharging/fuelling must be easy.* A single VTOL aircraft picks up the equipment from base and delivers the payload. It reaches back to the base station for another mission. The VTOL aircraft must be capable of performing three to four deliveries without a break. It must be easily rechargeable. The time taken to completely charge the VTOL aircraft should be minimum as time plays the most important role during a war.

4. *Send signals to ensure protocols of Geneva convention.* During a war like situation, any device or personnel providing medical aid to the wounded must not be attacked. Hence, our VTOL aircraft must be able to send radio signals to alert both armies to facilitate the vehicle passage through the area to the injured person. The VTOL aircraft will also be able to alert officials during survey of any suspected area about the presence of wounded personnel.[5]

5. *Ability to have a level flight at very low and high altitudes.* Battles often occur in densely forested areas on mountainous terrains. The VTOL aircraft must be capable of cruising at constant altitude to escape through the gaps in between trees. It is necessary that the VTOL aircraft could perform a level flight at a wide range of altitudes.

6. *Must be able to operate in confined spaces.* As mentioned earlier, the VTOL aircraft is to escape through minimum gaps in a dense environment of obstacles. It must be able to take off and land vertically, transition with minimal movement etc. Since the airstrip area to take off/ land cannot be available at all terrains and conditions, vertical takeoff and landing is necessary for this vehicle.

7. *Suitable for wind profile near a mountain.* Wind profile plays a major role in the range attained by an aircraft, and the time it takes to finish its mission. The VTOL aircraft is supposed to traverse through any wind profile within the stipulated mission time.

8. *Payload drop mechanism.* We wish to develop a mechanism to lower the payload from the VTOL aircraft at a small altitude from the ground, in the case landing is not possible. This is highly advantageous, as the chances of failure during landing on unpredictable terrains is reduced and can allow for faster delivery and return to base.

9. *Easily accessible payload area.* Easy accessibility of the payload bay is necessary to remove and replace the payload with ease quickly and without difficulty by operators/victims.

10. *Detecting heat signatures and distress signals - hand motion, etc.* We would like the VTOL aircraft to be controlled in a semi-autonomous

manner. There may be circumstances under which the pilot does not have accurate prior knowledge of the location of the victim/person requiring medical assistance. In such cases, the VTOL aircraft would be able to detect humans in distress using heat signatures or particular motion using hands, or SOS signals. This would help the VTOL aircraft to complete its mission in adverse situations too.

SNo.	Design Parameter	Value
1	Maximum Endurance	1.5 hours
2	Maximum Range	150 Km
3	Cruise Altitude	5100 m
4	Cruise Velocity	25 m/s
5	Maximum Velocity	25 m/s

1.5 Mission Profile and Segments

The following are the mission profile segments for this VTOL UAV:

1. **Takeoff:** This is a segment where the UAV takes off vertically with the help of rotors we will be having on board.
2. **Transition:** After reaching a desired height and initial velocity, the vertical rotors are stopped and horizontal motion starts. In this phase, the horizontal speed increases from zero to cruise speed.
3. **Cruise (forward):** It's the phase of the flight where it travels the desired distance (range) reaching the target region.
4. **Loiter(Hover and Delivery):** As per the mission our UAV is supposed to hover over the targeted region and drop the medical package(with the help of some dropping mechanism) to the people in need. In this phase the UAV is first lowered to a certain height and then performs the task.
5. **Cruise (return):** After completing the task, the UAV traces its path back returning to the original place where it started.
6. **Transition:** It's the similar as the transition discussed previously, with horizontal velocity be brought down completely to zero and vertical

thrusters turned on balancing the weight giving the required vertical velocity for smooth landing.

7. **Landing:** After delivering at the targeted location, the UAV lands vertically at the base station with the help of the vertical rotors.

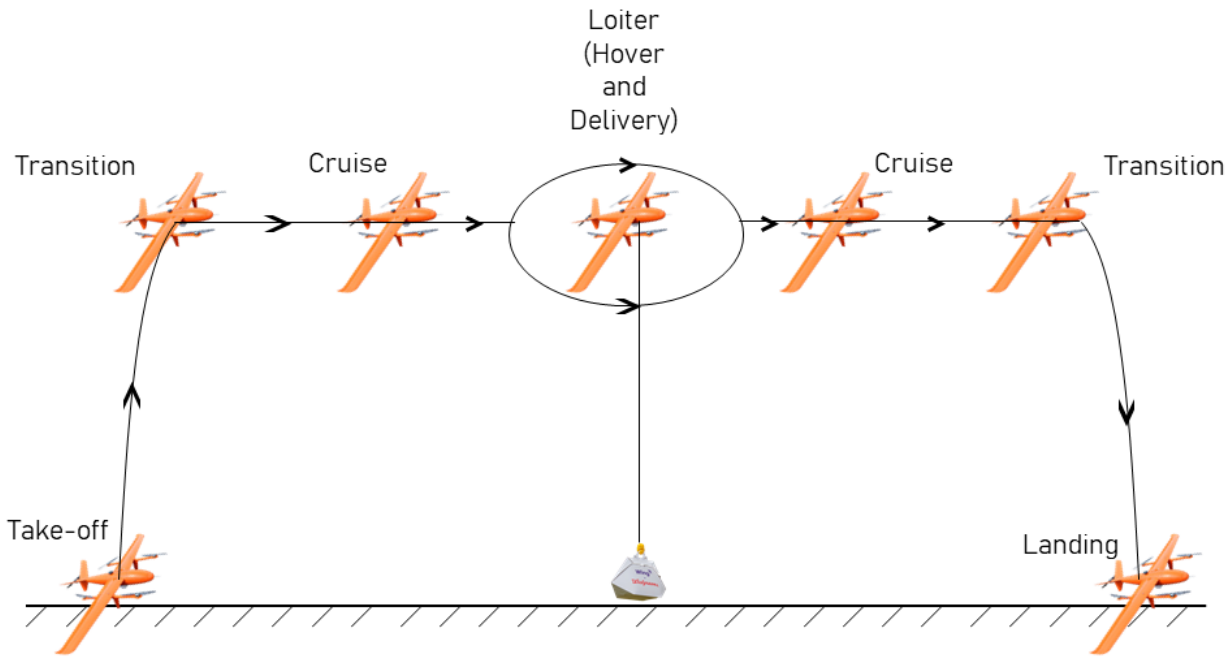

Figure 1.1: Mission Profile

SNo.	Name of Segment	Time	Distance	altitude
1	Take Off	90 s	0	0.1 km
2	Transition	30 s	-	-
3	Cruise (Forward)	1800 s	50 km	5 km
4	Loiter (Hovering and Delivery)	300 s	1 km	5 km
5	Cruise (Return)	1800 s	50 km	5 km
6	Transition	30s	-	-
7	landing	60s	0	0.1 km

[6]

Chapter 2

Weight Estimation

2.1 Weight Calculations

The total UAV weight is divided into 3 major sub-categories. These are:

- Battery weight $W_{battery}$
- Payload Weight $W_{payload}$
- Airframe weight(or empty weight) $W_{airframe} = W_e$. This includes the structural components, fixed equipment, avionics.

In order to get an estimate for the total weight of the aircraft, we need to know the empty weight and battery weight. But these are dependent on the total weight of aircraft. Thus, to find the weight of the UAV we need to adopt an iterative procedure. The process is as shown below

$$W_{overall} = W_{airframe} + W_{battery} + W_{payload}$$

$$W_{overall} = W_{overall} \times \frac{W_{airframe}}{W_{overall}} + W_{battery} + W_{payload}$$

$$W_o = \frac{W_{pay} + W_b}{1 - \frac{W_{af}}{W_o}} \tag{2.1}$$

Here, $W_o = W_{overall}$, $W_b = W_{battery}$, $W_{af} = W_{airframe}$, $W_{pay} = W_{payload}$.

The empty weight fraction(airframe weight fraction) is plotted against MTOW for aircraft collected in Appendix-A (Figure 2.1). We can observe a trend as follows:

$$\frac{W_{airframe}}{W_{overall}} = AW_{overall}^{C} \tag{2.2}$$

Where, A and C are constants and $C < 0$. From the fit, we obtained A and C as $A = 0.5963$ and $C = -0.0582$. This is done using MATLAB and the code is shown in Appendix-C

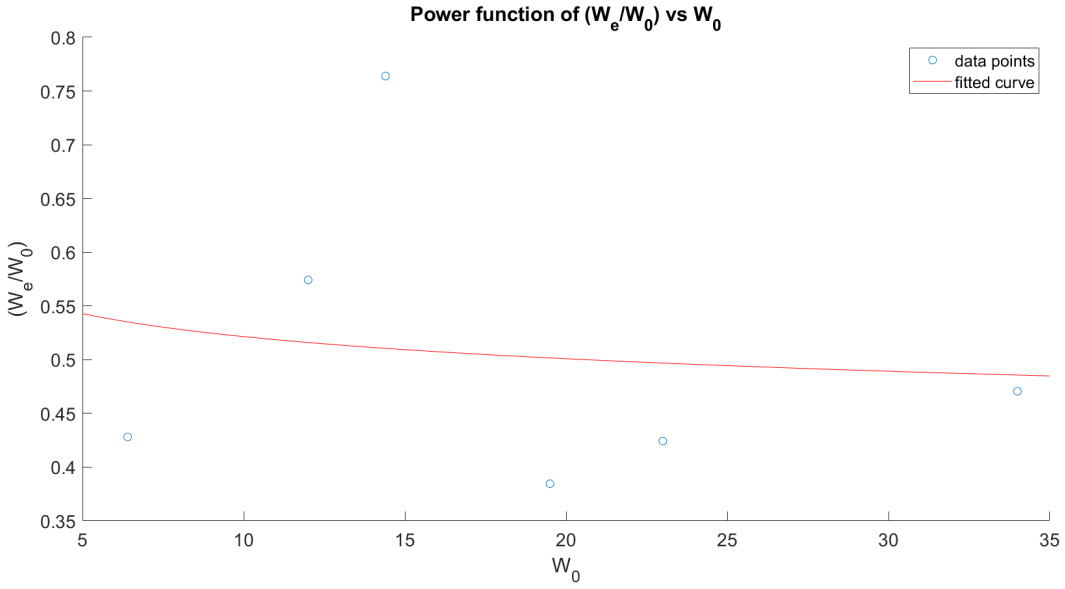

Figure 2.1: Empty weight fraction $\frac{W_e}{W_o}$ vs. overall weight (MTOW) W_o

2.2 Payload

2.3 Payload Weight

By comparing the weights of typical medical supplies and equipment (Table 2.1) used for primary response, we estimate the maximum payload weight of our VTOL to be **5 kg** including the mechanism for lowering the payload.

Component	Weight (kg)	Reference
Blood bag (450 ml)	0.48	[7]
First aid kit	0.45	[8]
Saline bag (500 ml)	0.5kg	[9]

Table 2.1: Weight of typical emergency medical supplies

While considering the mechanism for lowering the payload, we considered three options:

1. The VTOL lands and the payload bay (which is a temperature controlled box) is released.
2. The VTOL releases the payload box attached to a parachute.
3. The VTOL lowers the payload box to the ground using cables.

In the first approach, landing and taking off again will result in a large amount of battery power getting used up. Also, the terrain may not always be suitable for such a landing. The second approach has been used by companies such as Zipline [10] to deliver blood, however, the safety of the blood packet when they fall down, as well as the concern of parachutes getting stuck in densely forested areas and high speed winds make this approach less reliable and causes difficulty to the user (as they may need to recover the payload from a distant place). However, the advantage of this approach is that the drone need not lower its altitude, it can drop the parachute and fly to its next destination without delays and using the least amount of power. The third approach can work well even in densely forested areas and deliver the payload safely at the point of need with less effort from the user. This system has been successfully used by Google Wing [11] in their delivery drones. However, it may be difficult to stabilise the drone due to motion of the cables under strong winds. Hence, the VTOL may have to lower itself to a low altitude. Also, there could be a significant amount of additional weight due to the mechanism used to lower the payload. Considering the pros and cons of these approaches, we have decided to land the VTOL whenever the terrain is suitable, and use cables for lowering the payload from a maximum height of 10m. For initial estimation, the weight of the payload taking all these factors into account is considered to be 5kg.

2.4 Justification for preference of battery over fuel

For a drone to satisfy our mission statement, electric power offers a number of advantages. Few of which are listed below,

1. An electric motor is reliable because it has only one moving part. In addition, electricity is cheaper.
2. At an average of ten cents per kilowatt hour (kWh), the energy cost of an electric road vehicle is only one-quarter of that of a comparable gasoline-powered vehicle
3. Though there is a reduction in energy density, it is less severe for short-range aircraft. Also, the disparity in energy density is also partially compensated for by the substantially greater efficiency of the electric power system, particularly at a small scale: Small electric motors can be as much as nine times as efficient as comparable internal combustion (IC) engines
4. At delivery drone scales, electric motors have an eight-to-one advantage in specific power versus small IC engines

2.5 Energy and weight estimation of battery

Our initial weight estimate is 20kg. This weight includes the battery and payload weights. Now, considering other parameters from previous data, we have

Parameter	Symbol	Value	Unit
Aspect Ratio	AR	9.2	–
Wing Span	b	2	m
Empty Weight	W_e	28.33	kg
Take-off Weight	W_T	33.33	kg
Design Lift Coefficient	Cl	0.47	–
Cruise Speed	V_{cruise}	90	km/h
Taper Ratio	k	0.78	–
Wing Twist	–	- 1	Degree
Airfoil – NACA 63-512	a = 0.4	–	-
Maximum lift coefficient	CL_{max}	1.318	-
Parasite drag	C_{D0}	0.0447	–
Wing area	S_{wing}	0.485	m^2
Density at sea level	ρ_{SL}	1.225	$\frac{kg}{m^3}$
Ostwald efficiency factor	e	0.778	-

The steps used in the analysis given below[12] is written in a MATLAB Code which is shown in Appendix - B

2.5.1 Mission

We divided the mission segments into phases, and each phase power is calculated. The entire energy required is summed up multiplying the time taken in each phase with the power in each phase. The Mission sequence is as follows:

Name of segment	time	distance	altitude from MSL	initial vel(m/s)	final vel(m/s)
take off	90 s	0	5000 m	0	25
transition	30 s	-	5100 m	-	-
cruise (forward)	30 min.	50 km	5100m	25	25
loiter (hovering and delivery)	5 min.	1 km	5100m	25	25
cruise (return)	30 min.	50 km	5100m	25	25
transition	30 s	-	5100 m	-	-
landing	60 s	0	5100m	25	0

The steps used in the analysis given below[12] is written in a MATLAB Code which is shown in Appendix - B

2.5.2 Power required for take-off

The power required of rotor craft can be derived based on momentum theory on rotor disk. For vertical take-off and landing the ratio of thrust to weight K_T needs to be greater than one. We take K_T equal to 1.2.

$$P_{TO} = \frac{T_{TO} V_{TO}}{2} \left(1 + \sqrt{1 + \frac{2T_{TO}}{\rho V_{TO}^2 A_{Prop}}} \right)$$

$$T_{TO} = K_T W_{TO}$$

where V_{TO} is the take off velocity, and A_{Prop} is the propeller disc area. Here we take a commercially available propeller which is of 10 inch(25.4 cm) diameter. On substituting the values, we get

$$P_{TO} = 1.3358 \times 10^4 W$$

2.5.3 Power required for Transition from Take-off to Cruise

During transition, the vertical thrusters are stopped and the horizontal thrusters are turned on to accelerate from 0 to V_{cruise}. Thus, as a crude approximation we take the average power to be the power required to cruise at speed of

$V_{cruise}/2$.

$$P_{Transition} = \frac{1}{2}\rho S C_D \left(\frac{V_{cruise}}{2}\right)^3$$

where ρ is the density at the altitude, S is wing area and C_D is the total drag coefficient. Density at an altitude of 5100m is 0.7282 kg/m^3.(calculated using `atmosisa()` function in MATLAB)

$$C_D = C_{D0} + \frac{1}{\pi A R e} C_L^2$$

$$C_D = 0.0447 + \frac{1}{(3.14)(9.2)(0.778)}(0.47)^2 = 0.0545$$

$$P_{Transition} = 18.8048W$$

This is also valid for transition from return cruise to landing

2.5.4 Power required for cruise

Power is required in cruise to overcome drag losses.

$$P_{cruise} = \frac{1}{2}\rho S V^3 C_D$$

$$P_{cruise} = 150.4383W$$

This is applicable for both forward and return cruise.

2.5.5 Power required for Loiter

The loiter is approximated as a level flight of aircraft of weight equal to its takeoff weight. Thus, the power required is same as that of the cruise phase which is

$$P_{Loiter} = 150.4383W$$

2.5.6 Power Required for Hovering

The aircraft will be hovering using the VTOL rotors for about 30 s(when package is being dropped). This hovering power is calculated using the below

expression. Here we assumed that the UAV has 8 rotors

$$P_{Hover} = 4 \times \frac{T}{FoM}\sqrt{\frac{T}{2\rho A}}$$

Here $T = \frac{W}{4}$ and A is area of rotor disc and $FoM = 0.7$ is figure of merit.(More detailed explanation in chapter 3)

On substituting the values we get:

$$P_{Hover} = 5.1097 \times 10^3 W$$

2.5.7 Power required for descent

A descent velocity of $V_{Des} = 4$ m/s was suggested in this paper, and then the propellers are working on a condition of low speed axial descent $V_{Des} < 2V_H$. Assuming the variable x = -V_{Des}/V_H, the actual induced velocity V_i at the propeller disk can be given by the quartic approximation given as

$$V_i = (1.2 - 1.125x - 1.372x^2 - 1.718x^3 - 0.655x^4)V_H$$

$$V_H = \sqrt{\frac{T_{Hover}}{2\rho_{SL}A_{Prop}}}$$

$$T_{Hover} = W_{landing}$$

$$x = \frac{-V_{Des}}{V_H}$$

$$P_{Landing} = 1.2W_{landing}(V_i - V_{Des})$$

On substituting the values, we get:

$$P_{Landing} = 9.5098 \times 10^3 W$$

2.5.8 Energy requirements of the mission

So, the total energy requirement for the mission is

$$2577.4KJ = 715.9583Wh$$

The weight of a 22000mAh 22.2V LiPo battery (Energy = $\frac{\texttt{Charge in mAh} \times V}{1000}$ = $\frac{22000 \times 22.2}{1000}$ =488.4 Wh) is 2.604kg.[13] We use 3 batteries (total energy =

Name of the segment	time(s)	Power(W)	Energy(KJ)
take off	90	13358	1202.2
transition	30	18.8408	564.1438
cruise (Forward)	1800	150.4383	270.79
loiter	300	150.4383	45.132
Hover	30	5109.7	153.29
cruise (Return)	1800	150.4383	270.79
transition	30	18.8408	564.1438
Landing	60	9509.8	570.59

1465.2 Watt-hour) here and hence the total battery weight is 7.8120kg. We are using slightly higher power batteries here because they are commercially available and to account for efficiencies, change in weight in future iterations and dropping mechanism power.

2.6 Battery Power Variation with temperature

Since we are operating at high altitudes and low temperatures, we need to consider the changes in battery performance. Figure 2.2 shows the discharge performance v/s temperature for a LiPo battery [14].

Average temperatures at the Siachen base camp is between $-25°C$ during day and $-55°C$ during the night. At such low temperatures, the battery performance is severely affected. A possible solution to this is to heat up the batteries while charging to $20°C$, and then provide insulation to keep the batteries at a temperature above $0°C$, under which condition we get above 90% discharge efficiency. For this purpose, we choose to use silica gel insulation, as it is proven to be the best choice for LiPo batteries [15]. The loss in efficiency up to 90% have been considered in the power estimation.

2.7 First weight estimation

Now, we know that the battery weight from the previous section is $W_b = 7.812kg$ and the empty weight fraction is $\frac{W_e}{W_o} = 0.5963W_o^{-0.0582}$.We take the maximum payload weight as 5kg. On substituting these values in equation(2.1) we get:

$$W_o = \frac{W_{payload} + W_{battery}}{1 - \frac{W_e}{W_o}} = \frac{12.812kg}{1 - 0.5963W_o^{-0.0582}} \tag{2.3}$$

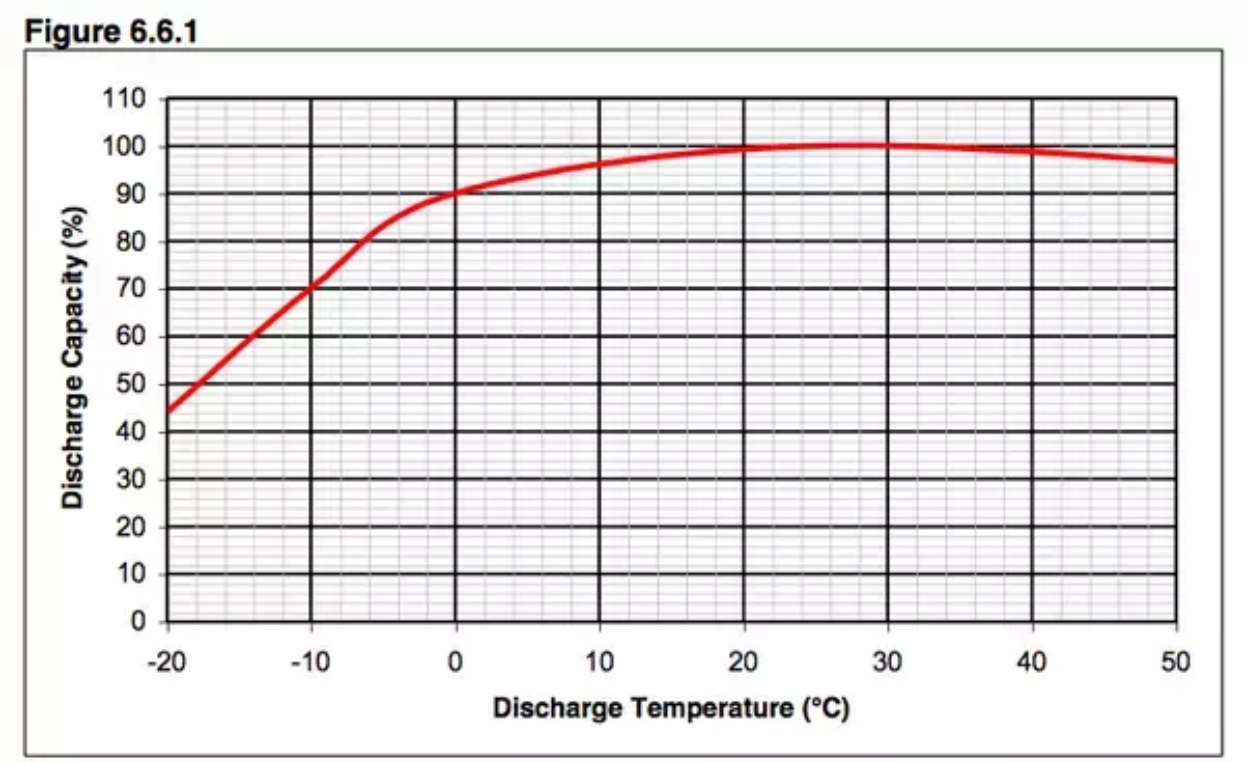

Figure 2.2: LiPo battery discharge performance (in %) against temperature

To solve this equation we use fixed-point iteration method. A sample calculation of this process is shown in section(2.7.1)

2.7.1 Sample calculation for first iteration

Assume an initial guess for $W_o|_0 = 20kg$. We use fixed-point iterations here to solve equation(2.3).

$$W_o|_{n+1} = \frac{12.812kg}{1 - 0.5963W_o|_n^{-0.0582}}$$

where $W_o|_i$ =MTOW after i iterations.

The RHS of the above equation after 1st iteration is

$$\frac{12.812kg}{1 - 0.5963W_o|_0^{-0.0582}} = 25.6698kg$$

.

Therefore, the weight to be used for 2^{nd} iteration is $W_o|_1 = 25.6698kg$ This weight is used to calculate weight to be used at 2^{nd} iteration and this process

is continued till convergence is achieved.

2.7.2 Convergence Plot

The analysis is done using MATLAB and the weight obtained at every iteration is plotted against iteration counter. The convergence plot is shown in figure(2.3). The MATLAB code used for obtaining this plot and weight estimate is shown in Appendix - C

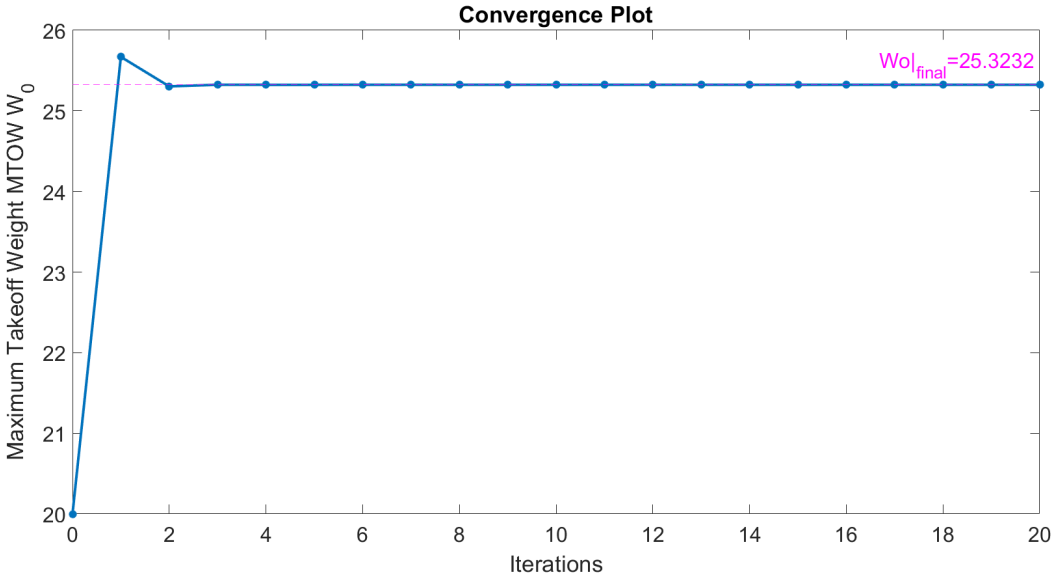

Figure 2.3: Convergence Plot

From the plot,we can see that the weight W_o has converged to $W_o = 25.3232kg$. In general 5% is added to this converged solution to account for weights of any missing components

Thus, the first weight estimate(MTOW) of the aircraft is

$$W_o = 1.05 \times 25.3232kg = 26.5893kg$$

2.8 Calculation of battery power from this first weight estimate

Using this MTOW, battery power consumed is calculated by following the same procedure in section 2.3. The power consumed is found out to be 1040.3 Wh.

If we assume that battery efficiency is 90% then the available power is $1465.2 \times 0.9 = 1318.7$ Wh. Thus, the excess power is $1318.7 - 1013.3 = 278.4$ Wh. This power may be used for dropping mechanism and any additional redundancies.

Chapter 3

Wing Loading, Power Loading & Disc Loading

To determine the wing loading of the aircraft, we consider the following constraints that the aircraft must satisfy to successfully complete the mission:

- Cruise speed
- Absolute Ceiling
- Rate of climb
- Stall speed

We have used the following data from existing similar aircraft,

Parameter	Symbol	Value	Unit
Aspect Ratio	AR	9.2	–
Oswald efficiency factor	e	0.778	–
Wing Span	b	2	m
Maximum Take-off Weight	W_o	18.6432	kg
Design Lift Coefficient	Cl	0.47	–
Cruise Speed	V_{cruise}	90	km/h
Taper Ratio	k	0.78	–
Wing Twist	–	- 1	Degree
Maximum lift coefficient	CL_{max}	1.318	-
Parasite drag	C_{D0}	0.0447	–
Wing area	S	0.485	m^2
V. tail area	S_{vtail}	0.055	m^2
H. tail area	S_{htail}	0.07	m^2
Wing wetted area	S_{wet}	0.821	m^2
Chord length	c	0.2425	m
Dynamic Viscosity	ν	1.789×10^{-5}	Pas
Density at 5100m	ρ_{SL}	0.7282	$\frac{kg}{m^3}$
[12]			

3.0.1 Approximating the drag polar

To approximate the drag polar we again take the dimensions from aircraft with similar takeoff weight and mission profile given in the table above.

Equation for Reynold's number is-

$$Re = \rho \times V_{cruise} \times \frac{c}{\nu}$$

$$Re = 0.728 \times 25 \times \frac{0.2425}{1.789 \times 10^{-5}} = 2.4677 \times 10^5$$

Equation for Equivalent skin friction drag coefficient-

$$C_{fe} = (2 \times log_{10}(Re) - 0.65)^{-2.3}$$

$$C_{fe} = (2 \times log_{10}(2.4677 \times 10^5) - 0.65)^{-2.3} = 0.00486$$

Equation for K_t is given by,

$$K_t = 1 + \frac{S_{vtail}}{S} + \frac{S_{htail}}{S} = 1.2577$$

Equation for Drag polar,

$$C_D = C_{D0} + C_{Di} = F_1 + F_2 p + F_3 P^2$$

Where,

$$F_1 = K_t C_{fe} \frac{S_{wet}}{S} = 0.01035N$$

$$F_2 = \frac{(C_{D0} - F_1)_W}{(W/S)_{old}} = 8.9367 \times 10^{-4} m^{-2}$$

$$F_3 = \frac{1}{\pi A R q^2 e} = 8.5878 \times 10^{-7} m^4 N^{-1}$$

S.No	Symbol	Value
1	F_1	0.01035 N
2	F_2	$8.9367 \times 10^{-4}\ m^2$
3	F_3	$8.5878 \times 10^{-7}\ m^4 N^{-1}$

3.0.2 Wing loading based on Cruise Constraint

Thrust loading and wing loading are related by the following equation,

$$\bar{t_v} = \frac{T_{vp}}{W} = \frac{C_D q_o}{p} = \frac{q_o}{p}(F_1 + F_2 p + F_3 p^2)$$

Power loading is given by the following,

$$\bar{p_v} = \frac{P}{W} = \frac{T_{vp} V}{W \eta_{prop}} = \frac{\bar{t_v} V}{\eta_{prop}}$$

On simplifying further we get,

$$\bar{p_v} = q_o V \frac{\frac{F_1}{p} + F_2 + F_3 p}{\eta_{prop}}$$

To get the optimum value of wing loading (p) for minimum value of $\bar{p_v}$ we take the derivative of $\bar{p_v}$ with respect to wing loading p,

$$\frac{d\bar{p_v}}{dp} = q_o \frac{V}{\eta_{prop}}(\frac{-F_1}{p^2} + F_3) = 0$$

$$p = \sqrt{\frac{F_1}{F_3}} = \sqrt{\frac{0.01035}{8.5878 \times 10^{-7}}} = 109.78 N/m^2$$

In the figure given below optimum value of $\bar{p_v}$ is marked. Taking 5% increase in the minimum p calculated, we get two values of wing loading as follows,

1. $160.95 kgm^{-1}s^{-2}$
2. $74.7 kgm^{-1}s^{-2}$

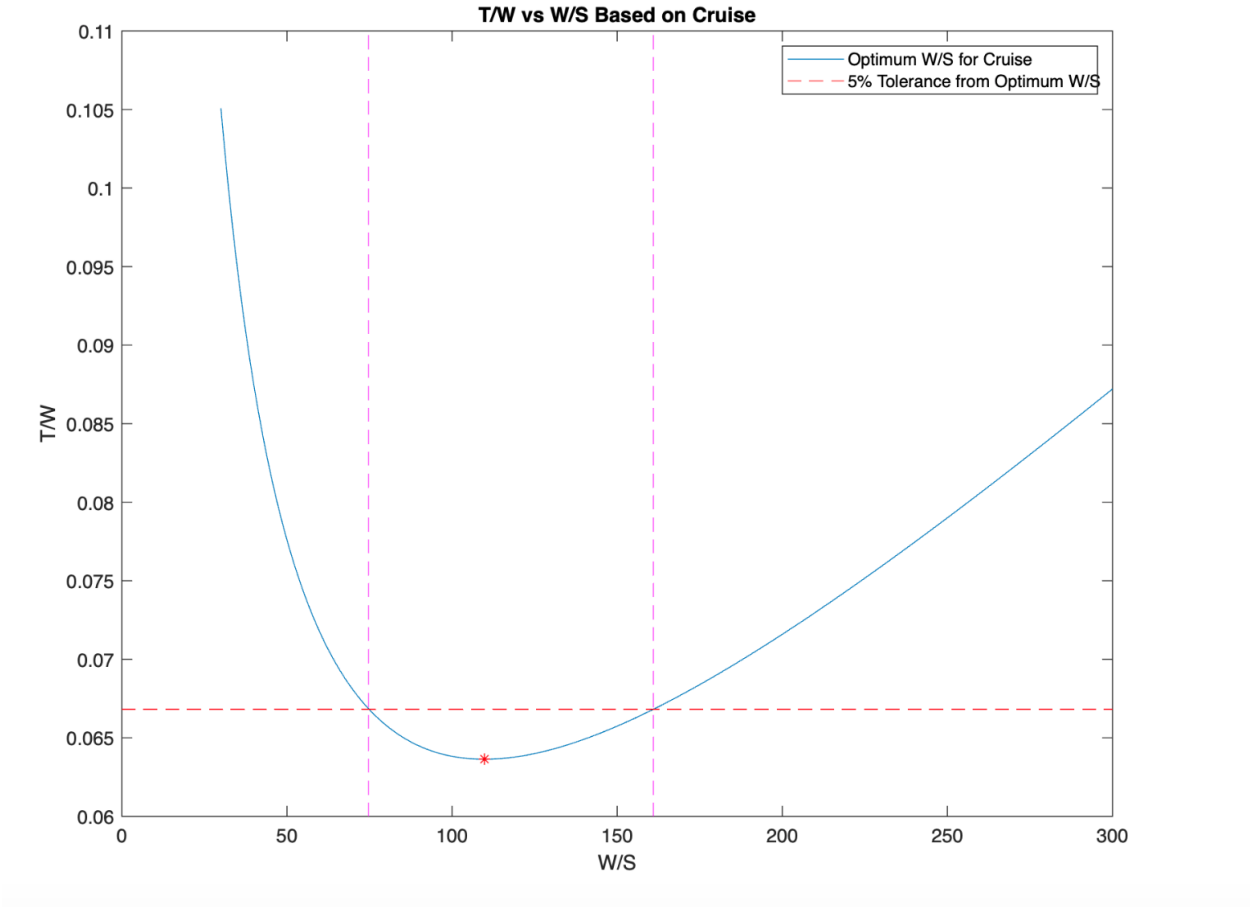

Figure 3.1: Optimal W/S for Cruise

3.0.3 Wing loading based on Absolute Ceiling Constraint

At absolute ceiling the flight is possible only at one speed at which T_{req}(Required Thrust) = T_{min}(Minimum Thrust) = D_{min}(Minimum drag). Hence, for an aircraft at absolute ceiling (i.e. at maximum altitude at which it can maintain level flight)

$$\bar{t}_{Hmax} = \frac{D_{min}}{W} = \frac{1}{(L/D)_{max}} \tag{3.1}$$

Considering the parabolic drag polar $C_D = C_{D_0} + KC_L{}^2$ We can obtain the maximum by differentiation the value obtained are as follows:

$$(C_L)_{(L/D)_{max}} = (C_{D_0}/K)^{\frac{1}{2}} \tag{3.2}$$

$$(C_D)_{(L/D)_{max}} = 2C_{D_0} \tag{3.3}$$

Therefore,

$$\bar{t}_{Hmax} = \frac{1}{(L/D)_{max}} = \sqrt{4C_{D_0}K}$$

Also as we have found that $C_{D_0} = F_1 + F_2 p$, where, $F_1 = 0.01035$, $F_2 = 8.9367 \times 10^{-4}$

The Thrust loading will now be given as

$$\bar{t}_{Hmax} = \sqrt{4(F_1 + F_2 p)K} \tag{3.4}$$

The power loading can be calculated as follows

$$\bar{p_v} = \frac{P}{W} = \frac{T_{vp}V}{W\eta_{prop}} = \frac{\bar{t_v}V}{\eta_{prop}}$$

$$\bar{p_v} = \frac{V\bar{t}_{Hmax}}{\eta_{prop}} \tag{3.5}$$

$$\bar{p_v} = \frac{V\sqrt{4(F_1 + F_2 p)K}}{\eta_{prop}} \tag{3.6}$$

We have plotted the above eqation in the figure below. We can observe that the thrust loading increases with wing loading in this case.

Sometimes, the flight velocity (V_{Hmax}) may be prescribed at absolute ceiling. In this case, the optimization of wing loading is carried out in the following manner. Note that $q_{Hmax} = \frac{1}{2}\rho_{Hmax}V_{Hmax}^2$

$$\bar{t}_{Hmax} = \frac{D_{min}}{W} = \frac{q_{Hmax}S(C_D)_{(L/D)_{max}}}{W} \tag{3.7}$$

from eqn 3.3 we have $(C_D)_{(L/D)_{max}} = 2C_{D_0}$. substituting $C_{D_0} = F_1 + F_2 p$, we get

$$\bar{t}_{Hmax} = 2q_{Hmax}(\frac{F_1}{p} + F_2) \tag{3.8}$$

The power loading will then be given as

$$\bar{p_v} = \frac{2V_{Hmax}q_{Hmax}}{\eta_{prop}}(\frac{F_1}{p} + F_2) \tag{3.9}$$

We have plotted above equation in the figure below. We can observe that the thrust loading decreases with wing loading in this case. It can be seen that at one point both the plots intersect. That is the optimum point which gives us optimum wing loading amd corresponding thrust loading. Allowing as deviation from the optimum value, the permissible upper and lower limits on p are obtained.

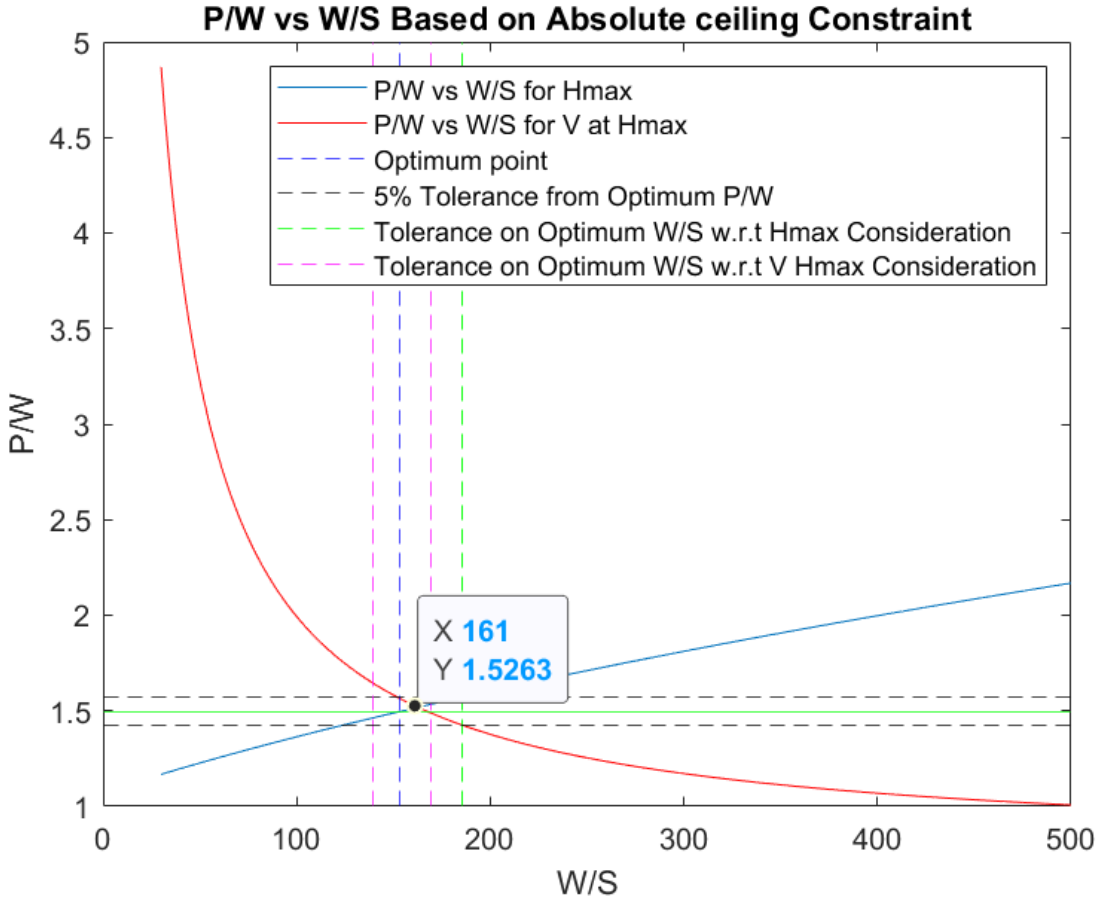

Figure 3.2: Optimal W/S for Absolute ceiling

3.0.4 Wing loading based on Rate of Climb

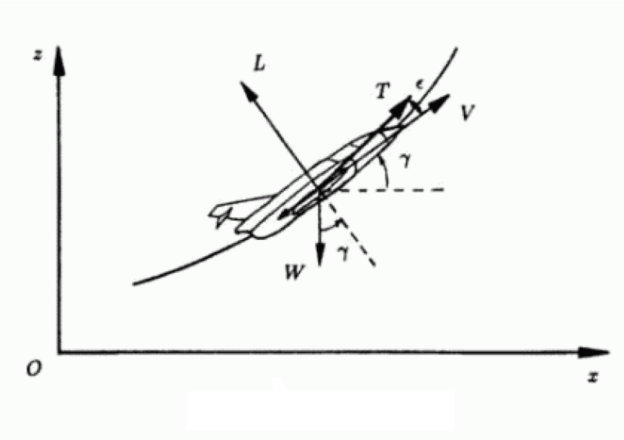

Figure 3.3: Aircraft in climb flight

We know that in climb flight (Figure 3.3), the rate of climb V_z

$$V_z = V \sin\gamma = V\frac{T_a - D}{W} \tag{3.10}$$

where V is the velocity, γ is the climb angle, T_a is the thrust available, D is the drag and W is the weight of the aircraft (maximum takeoff weight to be considered here). Denote $\frac{T_a}{W}$ by $t_{R/C}$, representing the thrust loading. We know $D = \frac{1}{2}\rho V^2 S C_D$, where S is the area of the wing and C_D is the drag coefficient. Define the wing loading $p = \frac{W}{S}$. Hence, 3.10 becomes:

$$V_z = V(t_{R/C} - \frac{1}{2}\rho V^2 \frac{C_D}{p}) \tag{3.11}$$

Rearranging we get,

$$t_{R/C} = \frac{V_z}{V} + \frac{1}{2}\rho V^2 \frac{C_D}{p} \tag{3.12}$$

The drag coefficient can be approximated as:

$$C_D = F_1 + F_2 p + F_3 p^2 \tag{3.13}$$

then we can write:

$$\begin{aligned} t_{R/C} &= \frac{V_z}{V} + \frac{1}{2}\rho V^2(\frac{F_1}{p} + F_2 + F_3 p) \\ &= \frac{V_z}{V} + \frac{1}{2}\rho V^2 \frac{F_1}{p} + \frac{1}{2}\rho V^2 F_2 + \frac{Kp}{\frac{1}{2}\rho V^2}) \end{aligned} \tag{3.14}$$

From this equation we can see that the thrust loading is a function of V and wing loading p. Hence, to minimise the thrust loading, we need to satisfy $\frac{\partial t_{R/C}}{\partial V} = 0$ and $\frac{\partial t_{R/C}}{\partial p} = 0$. Doing so, we get [16]:

$$\begin{aligned} V_o pt &= (\frac{V_z}{\rho F_2})^{1/3} \\ p_{opt} &= \frac{1}{2}\rho V^2 \sqrt{\frac{F_1}{K}} \\ \implies p_{opt} &= \frac{1}{2}\rho (\frac{V_z}{\rho F_2})^{2/3} \sqrt{\frac{F_1}{K}} \end{aligned} \tag{3.15}$$

Substituting the above in equation 3.14, we get:

$$t_{R/C} = \frac{V_z}{V_{opt}} + \frac{1}{2}\rho V_{opt}^2 \frac{2F_1}{p_{opt}} + F_2 \tag{3.16}$$

For our aircraft, the takeoff time is 90s, and the altitude achieved during takeoff with respect to the base camp is 100m. Hence, the rate of climb suitable for our mission is:

$$V_z = \frac{100m}{90s} = 1.11 m/s$$

Using this value and the above analytical results, we can obtain:

$$\begin{aligned} V_{opt} &= 25.5858 m/s \\ p_{opt} &= 173.6156 N/m^2 \\ t_{R/C} &= 0.1080 \end{aligned}$$

We can also plot $t_{R/C}$ against p_{opt} for different V and obtain the absolute

minimum numerically. The values corresponding to this are:

$$V_{opt} = 26m/s$$
$$p_{opt} = 118N/m^2$$
$$t_{R/C} = 0.1081$$

We can observe that the theoretical and actual values are in close agreement. The p_{opt} values show significant differences in both the cases; this can be attributed to the flatness of the curves near minimum value, and to the fact that the numerical calculations are highly approximate. Due to the flatness of the curve near minimum, a 5% increase in the $t_{R/C}$ value can be allowed. Corresponding to this and our numerical calculations, we obtain the range of allowable wing loading as 71.1366 to $195N/m^2$ (Figure 3.4).

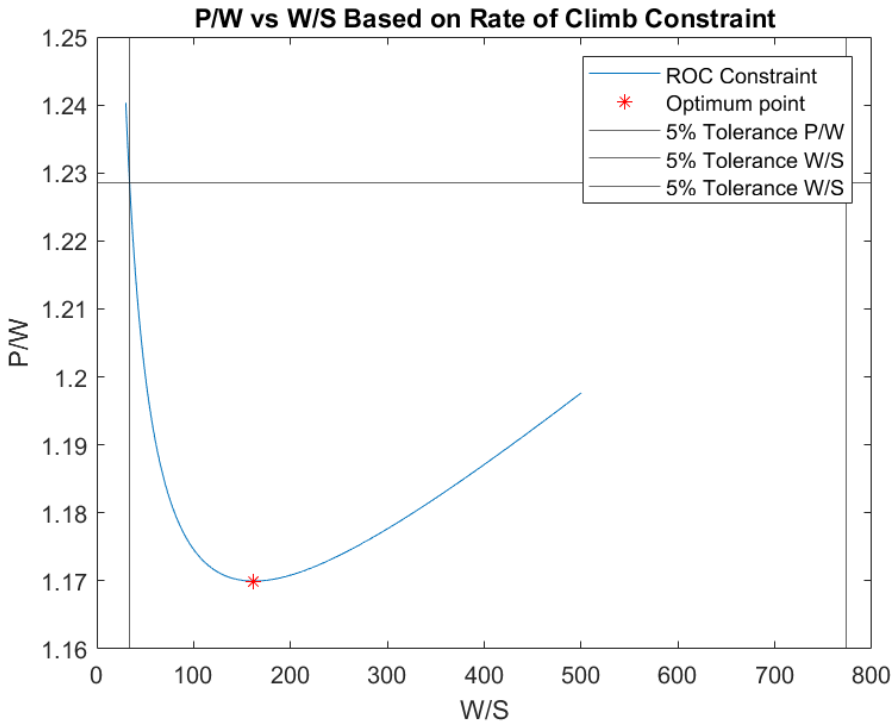

Figure 3.4: Wing Loading range based on Rate of Climb constraint

Based on the above calculations, the final constraint diagram has been plotted (Figure 3.5) and the optimum values of power loading and wing loading have been determined. The design point has been determined by the stall constraint and the minimum power required. The optimum region can be

seen as the shaded yellow region. The optimum wing loading corresponding to the design point is:

$$\frac{W}{S} = 168.7091 n/m^2 \tag{3.17}$$

[17]

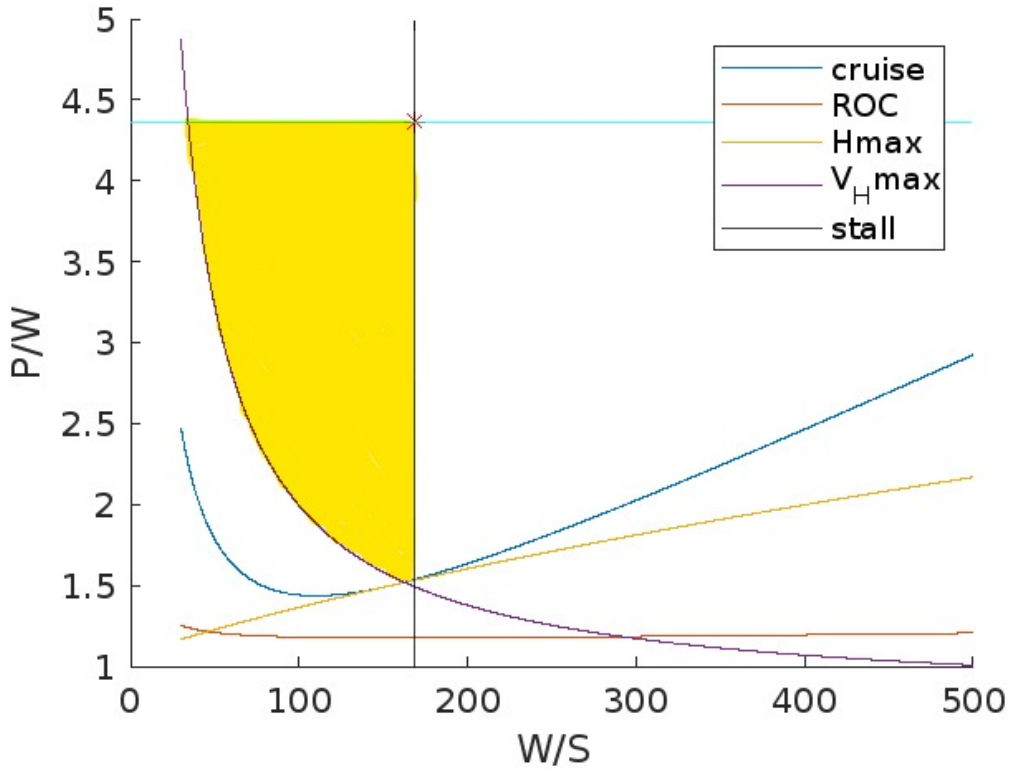

Figure 3.5: Final Constraint Diagram

3.1 Disc Loading

Disc loading (defined for an aircraft with rotors) is defined as the ratio of the thrust produced by a rotor to the area of the actuator disc i.e, $DL = \frac{T}{A}$.

The below analysis is given in [18] and coded in MATLAB. The MATLAB Code used is shown in Appendix - D

3.1.1 Hovering Flight

From the blade momentum theory, we know that the velocity induced by the rotor disc v_i and the ideal power required to hover P_i are given by equa-

tions(3.18),(3.19)

$$v_i = \sqrt{\frac{T}{2\rho A}} \tag{3.18}$$

$$P_i = Tv_i = T\sqrt{\frac{T}{2\rho A}} \tag{3.19}$$

where T is thrust produced by rotor $T = W/n$ (where n is number of rotors), ρ is density of air at hover altitude and A is the area of the actuator disc.

We typically add an induced power correction factor k_i to include any effects of non-uniform inflow, wake swirl, non-ideal wake contraction and the effect of finite number of blades on the aircraft. The average value of k_i in hovering is 1.15.

$$P_{i,non-ideal} = k_i P_i = k_i T\sqrt{\frac{T}{2\rho A}} \tag{3.20}$$

There is also the rotor profile power P_o, which is required to overcome the profile drag of the blades and is obtained by taking the drag of a blade element and integrating over the span of the blade

$$P_o = \frac{1}{8}\rho A V_{tip}^3 \sigma C_d \tag{3.21}$$

where C_d is the average blade drag coefficient, σ is the rotor solidity ratio (ratio between total blades area and rotor disc area), and V_{tip} is the rotor's tip speed.

Thus, the total actual power consumed by a rotor in hover is

$$P = P_{i,non-ideal} + P_o = k_i T\sqrt{\frac{T}{2\rho A}} + \frac{1}{8}\rho A V_{tip}^3 \sigma C_d \tag{3.22}$$

At this design stage, there is no precise data about a number of design parameters such as the rotor diameter, tip speed, airfoil type, solidity, drag, etc. which prevents the exact calculation of the power required for the rotor profile drag. To account for the power needed to overcome these effects, we define a quantity called **Figure of Merit**(FoM) which is the ratio of ideal induced power for a rotor in hover and the actual power consumed by the

rotor.

$$FoM = \frac{P_i}{P} \tag{3.23}$$

Typical values of FoM is 0.6 - 0.7. We take FoM = 0.7 here. We can also find P_o in terms of P_i as follows:

$$FoM = \frac{P_i}{P} = \frac{P_i}{k_i P_i + P_o}$$

$$P_o = P_i \left(\frac{1}{FoM} - k_i \right) \tag{3.24}$$

We can write power consumed by the rotor as:

$$P = \frac{T}{FoM} \sqrt{\frac{DL}{2\rho}} \tag{3.25}$$

As weight is W = kg and propeller disc is of diameter 10 inch(25.4 cm), we get the disc loading for each propeller disc as:

$$DL = \frac{T}{A} = \frac{W}{4A} = 1.2869 \times 10^3$$

And then using equation(3.25) we get the power required for each propeller as $P = 2.7543 \times 10^3 W$ and hence power required in hover segment is $4P = 1.1017 \times 10^4 W$.

Chapter 4

Wing design

4.1 Airfoil selection

The most important parameters in selecting airfoil section is the ideal airfoil lift coefficient C_{l_i} and the maximum airfoil section lift coefficient $C_{l_{max}}$. These can be calculated as follows:

From the wing loading calculations, we know that $W/S = 168.7091$. We can then find the aircraft ideal cruise lift coefficient as:

$$C_{L_C} = \frac{2W/S}{\rho V_c^2} = 0.7414 \tag{4.1}$$

where V_c is the cruise speed. Now, we need to find the wing cruise lift coefficient, the component of the aircraft cruise lift coefficient excluding the effect of other aircraft components. Since the geometry of these components has not yet been determined, we use an approximation [19]:

$$C_{L_{Cw}} = \frac{C_{L_C}}{0.95} \tag{4.2}$$

Now, the wing airfoil ideal lift coefficient has to be estimated. Since the wing sweep, dihedral, span, etc. has not yet been determined, we need to use an appproximation as [19]:

$$C_{l_i} = \frac{C_{L_{Cw}}}{0.9} \tag{4.3}$$

The maximum lift coefficient has been estimated from previous data to be [12]:

$$C_{L_{max}} = 1.318 \tag{4.4}$$

Using this we can find the wing maximum lift coefficient as:

$$C_{L_{max_w}} = \frac{C_{L_{max}}}{0.95} \tag{4.5}$$

and the wing airfoil net maximum lift coefficient as:

$$C_{l_{max}} = 1.5415 \tag{4.6}$$

Since in our design we do not require high lift devices, its contribution to the airfoil net maximum lift coefficient is zero. These calculations are performed using the code in E

Based on these values we choose an airfoil that provides $C_{l_{max}}$ higher than our required value and C_{l_i} close to our calculated value. Using an airfoil database [20], we found few airfoils satisfying our requirements:

Airfoil	$C_{l_{max}}$	C_{l_i}	$(L/D)_{max}$	C_{m_0}
GOE 13K	2.28	0.896	153.8	-0.202
GOE 164	1.94	0.85	111.202	-0.158
GOE 366	2.34	0.907	102.28	-0.156
GOE 390	2.71	0.881	89.715	-0.147
EPPLER 858	2.47	0.861	129.882	-0.155
EPPLER 857	2.21	0.826	149.338	-0.157
NACA 6418	2.36	0.878	89.347	-0.163

Table 4.1: Selected Airfoils

The criteria we use to select the airfoils are:

- Maximum $C_{l_{max}}$
- Closest C_{l_i} to calculated value
- Maximum $(L/D)_{max}$
- C_{m_0} closest to 0
- Easy to manufacture

Based on these criteria, EPPLER 858 is the chosen airfoil for our mission (Figure 4.1)

The characteristics of the airfoil selected are as shown in Figure 4.2 to Figure 4.6.

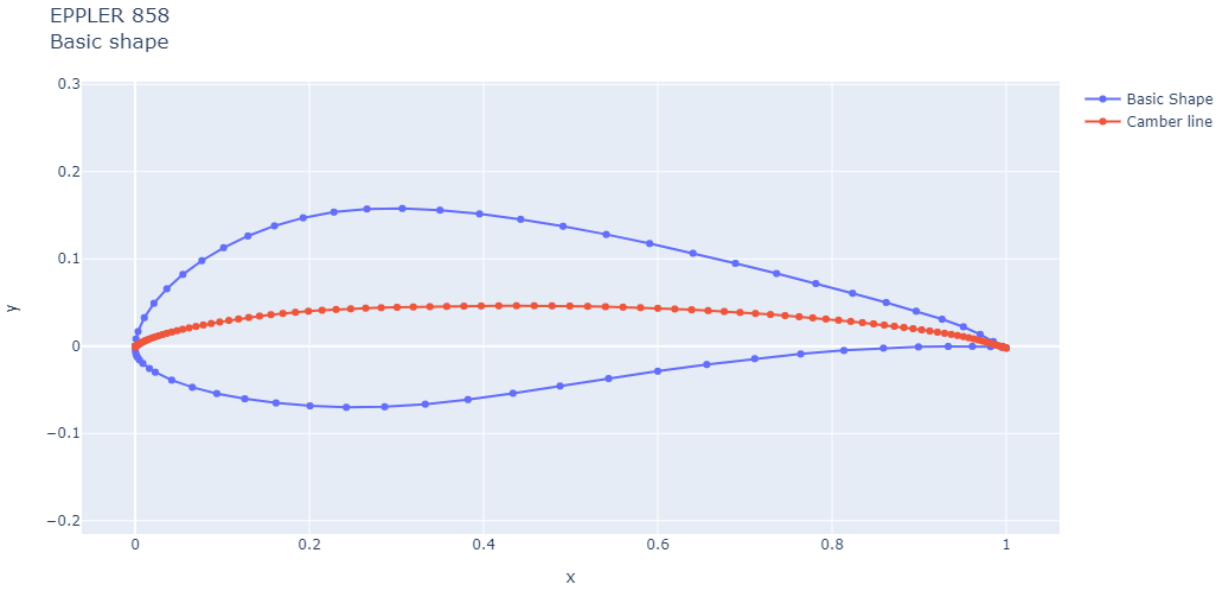

Figure 4.1: EPPLER 858

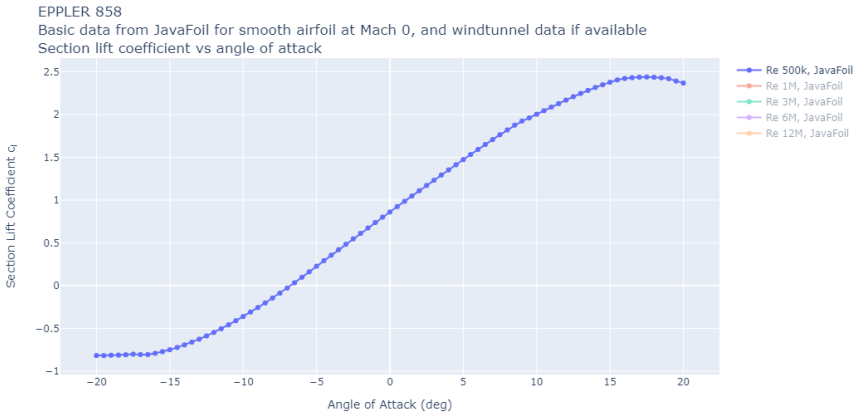

Figure 4.2: C_l v/s α

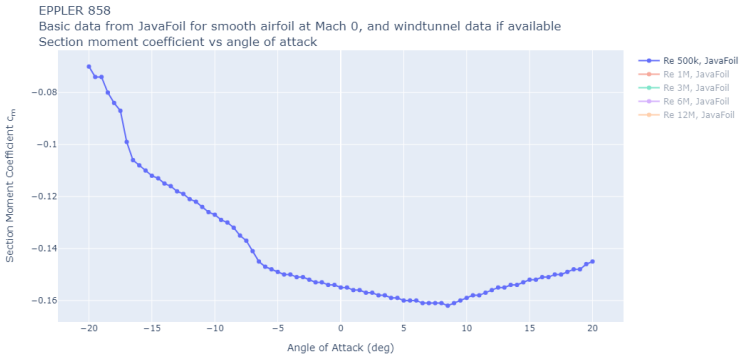

Figure 4.3: C_m v/s α

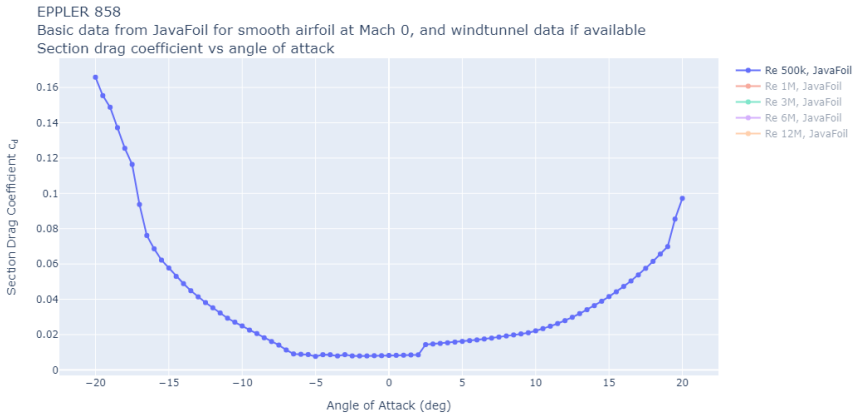

Figure 4.4: C_d v/s α

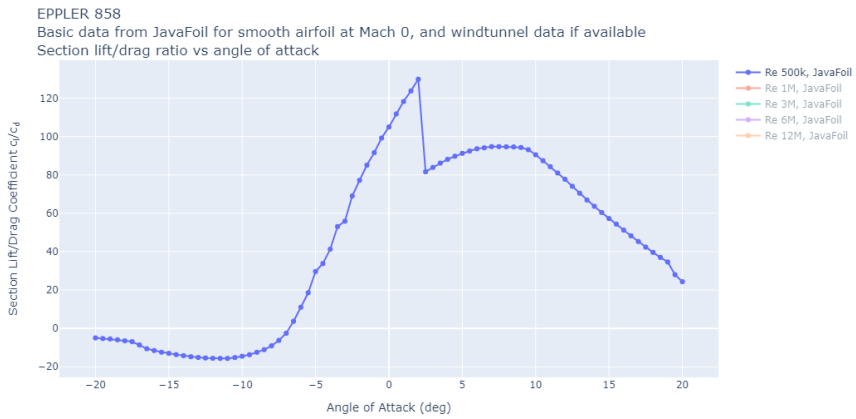

Figure 4.5: $\frac{C_l}{C_d}$ v/s α

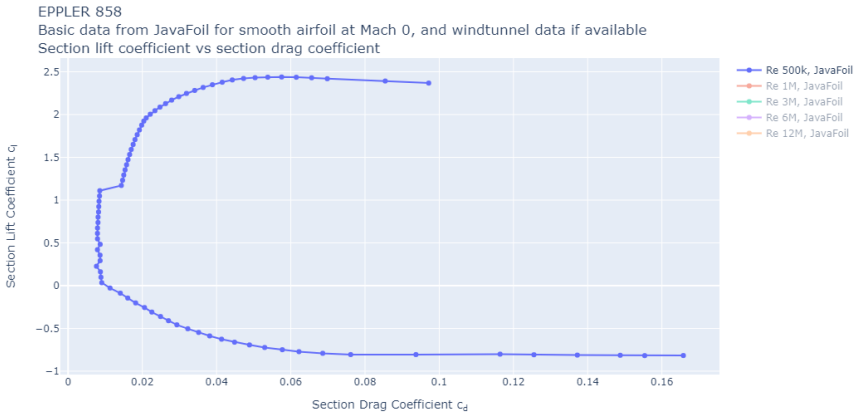

Figure 4.6: C_l v/s C_d

4.2 Wing Design

4.2.1 Number of Wings

An airplane can have a single wing(monoplane), 2 wings(biplane) and 3 wings(tri-wing). An airplane having more than 3 wings is impractical. The advantage for choosing more than one wing is to reduce wing span for high roll control. But the disadvantages are high weight and more drag. For our aircraft, we choose a single wing(i.e., Monoplane.)

4.2.2 Wing Vertical Location

There are 3 possible options for the vertical location of the wing - (1) High Wing; (2) Mid Wing; and (3) Low Wing.

1. **High Wing**

   Advantages

   (a) With a high wing,the propellers will have sufficient ground clearance without excessive landing-gear length.

   (b) The wing tips of a swept high wing are not as likely to strike the ground when in a nose-high, rolled attitude.

   (c) For low-speed aircraft, external struts can be used to greatly lower wing weight. This is because in case of high-wing, the struts handle tensile stress.

(d) The wing will produce more lift since two parts of the wing are attached at least on the top part.

(e) It provides roll stability

(f) Wing is not present in downwash of rotors.

Disadvantages

(a) Due to increase in the frontal area, the drag is higher in this configuration.

(b) While landing-gear weight tends to be lower than other arrangements, the fuselage weight is usually increased because it must be strengthened to support the landing-gear loads.

2. **Low Wing**

Advantages

(a) Aircraft has less frontal area and hence less drag.

(b) The landing gear is shorter if connected to the wing. This makes the landing gear lighter and requires less space inside the wing for the retraction system. This will further make the wing structure lighter

(c) The wing has less downwash on the tail, so the tail is more effective.

Disadvantages

(a) The wing generates less lift when compared to high-wing configuration as the wing has 2 separate sections. Due to this aircraft has less $C_{L_{max}}$ and hence, larger stall speeds.

3. **Mid Wing**

Advantages

(a) Aerodynamically, mid-wing plane is more streamlined when compared to other two configurations. Due to this, the mid-wing has less interference drag.

(b) Roll maneuvers can be performed quickly.

Disadvantages

(a) The aircraft structure is heavier, due to the necessity of reinforcing the wing root at the intersection with the fuselage.

(b) The mid wing is more expensive compared with high wing and low wing configurations.

From this list, we find that a high-wing configuration is the best for this aircraft.

4.2.3 Wing Area

From chapter 3, the wing loading is between and and . The optimum wing loading is 168.7091.

Thus, the wing area

$$S = \frac{W}{\frac{W}{S}} = \frac{26.5893 \times 9.81}{168.7091} = 1.5461 m^2$$

4.2.4 Aspect Ratio

Aspect ratio AR of the wing is defined as follows:

$$AR = \frac{b^2}{S} \tag{4.7}$$

where b is wing span and S is wing area. For this aircraft Aspect ratio is chosen as 11. This optimisation is done using Prandtl's lifting line theory.

4.2.5 Wing Span

We know that

$$AR = \frac{b^2}{S}$$

On rearranging, we get

$$b = \sqrt{AR \times S} \tag{4.8}$$

We know that $AR = 11$ and $S = 1.5461\, m^2$. On substituting these values we get $b = 4.1240\, m$. We can also find the mean aerodynamic chord $\bar{c}$ using the relation,

$$AR = \frac{b}{\bar{c}} \Rightarrow \bar{c} = \frac{b}{AR}$$
$$\therefore \bar{c} = 0.3749 \text{ m}$$

4.2.6 Taper Ratio & Twist

The taper ratio is defined as the ratio of tip chord length to root chord length.

A rectangular wing is considered here due to ease of manufacturing. Due to this, taper ratio = 1. Airfoil twist is also not given for the same reason.

4.2.7 Sweep

Sweep angle Λ is the angle between quarter chord line of the wing and line perpendicular to the center line.

The Mach number for this aircraft during cruise is

$$M = \frac{V_{cruise}}{\sqrt{\gamma RT}} = \frac{25}{\sqrt{1.4 \times 287 \times (273 - 50)}} \approx 0.084 < 0.3$$

As Mach number of the aircraft is less than 0.3(i.e., aircraft is in low subsonic regime), no sweep angle is recommended. (Though there is a slight reduction in drag for a swept wing, wing manufacturing complexity and cost increases.)

4.2.8 Dihedral angle

For the preliminary design, the dihedral angle Γ is chosen to be zero. This might change later after doing stability checks.

4.2.9 Wing incidence

Wing incidence angle i_w is the angle made by the wing chord and the fuselage reference line.

For a wing with zero twist

$$C_L = C_{L_\alpha}(i_w - \alpha_{L=0})$$

Here, C_L is the lift coefficient of the wing, C_{L_α} is the lift curve slope and $\alpha_{L=0}$ is the zero lift angle of attack.

On rearranging the above equation, we can get i_w as follows:

$$i_w = \alpha_{L=0} + \frac{C_L}{C_{L_\alpha}} \tag{4.9}$$

We can find the lift curve slope using the below equation:

$$C_{L_\alpha} = \frac{2\pi AR}{2 + \sqrt{4 + \frac{AR^2\beta^2}{\eta^2}(1 + \frac{\tan\Lambda_{1/2}}{\beta^2})}} \tag{4.10}$$

where,
$\beta = \sqrt{1 - M^2} = 0.9965$
$\eta = \frac{C_{l_\alpha}}{2\pi} = 1.1362$ for $C_{l_\alpha} = 0.1246/deg$
$\Lambda_{1/2} = 0 =$ sweep angle of mid chord
$C_{l_\alpha} = 7.1391/rad$

$$\therefore C_{L_\alpha} = 5.8312/rad$$

On substituting the values of $C_{L_\alpha} = 5.8312/rad$, $C_L = 0.7414$, and $\alpha_{L=0} = -6.77°$ in equation(4.9) we get $i_w = 0.5148°$

Chapter 5

Fuselage Sizing

5.1 Fuselage Length

For initial guidance during fuselage layout and tail sizing, we use a power-law relation between fuselage length and the take-off weight. [21]

$$\texttt{Fuselage length} = aW_0^c \tag{5.1}$$

The below table shows the fuselage lengths for aircraft used in Appendix-A

Aircraft	Weight W_0(kg)	Fuselage Length(in m)
Yangda FW-320	23	1.2
Yangda Sky Whale	34	1.92
Google Wing	6.4	1.3
EoSC	14.2	1.8
Avy Area New	19.5	1.5

Table 5.1: Fuselage Lengths for different aircraft

The power law(5.1) is fit for the data shown in table(5.1) in figure(5.1) (MATLAB code attached in Appendix-G) and we find out that $a = 1.0406$ and $c = 0.1337$. For the design weight the Fuselage length is calculated using the relation as shown below.

$$\texttt{Fuselage Length} = 1.0406 \times (26.5893)^{0.1337}\ m = 1.6137\ m$$

Therefore, the design fuselage length is approximately 1.614 m.

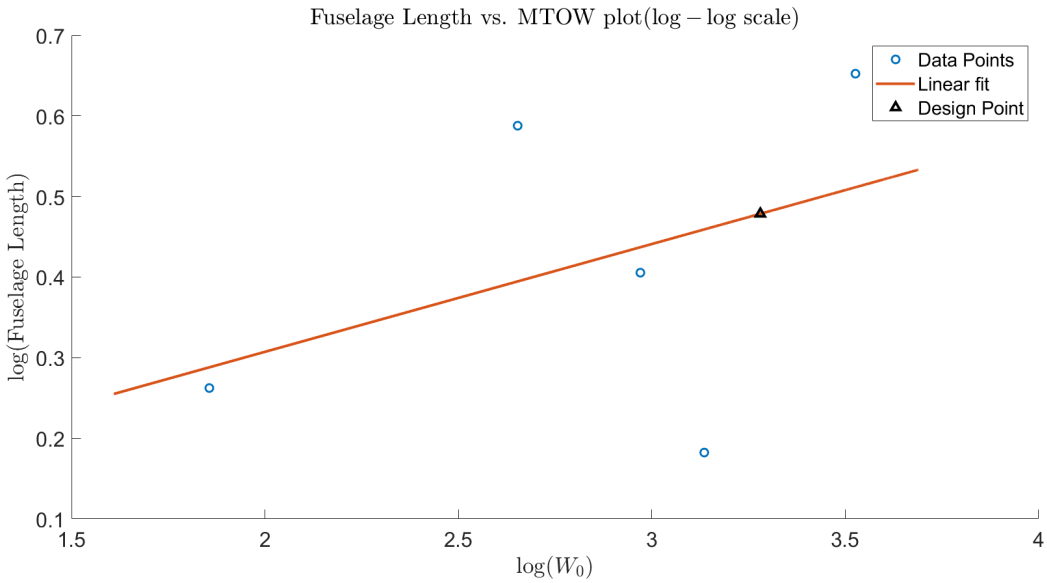

Figure 5.1: Linear fit of Weight (in kg) vs. Fuselage length(in m)

Chapter 6

Tail Design

The primary function of the tail is to trim the aircraft, provide stability and controlability.We have a variety of tail designs available such as conventional tail design, T-tail configuration, v-tail, H-tail.Now, there is no such things as high tail, mid-tail or low tail, unlike how it is for the wing case. But low tail basically implies horizontal tail, high tail implies T-tail type and mid tail implies cruciform type.
The components such as wing, fuselage acts as sources for the interference. The tail performance could be affected due to wing downwash, wakes and trailing vortices. The most important consideration in determining the location of the horizontal case is the prevention of deep stall. The horizontal tail location must not be in the wing wake region when the wing stall happens. The below figure shows the three possible locations. a) out of the wake region and downwash, b)inside the wake region but outside the wing downwash, c) out of the wake region but affected by the downwash.

Observing it carefully we realise that the region a) is the best as it is out of both downwash as well as the wakes. region c) is safe from deep stall and pitch up but the tail is not efficient. Region b) is not safe and not recommended for horizontal tail location. The initial approximation of the vertical tail should be as follows:

$$ht > tan(\alpha_s - i_w - 3) \tag{6.1}$$

$$ht < tan(\alpha_s - i_w + 3) \tag{6.2}$$

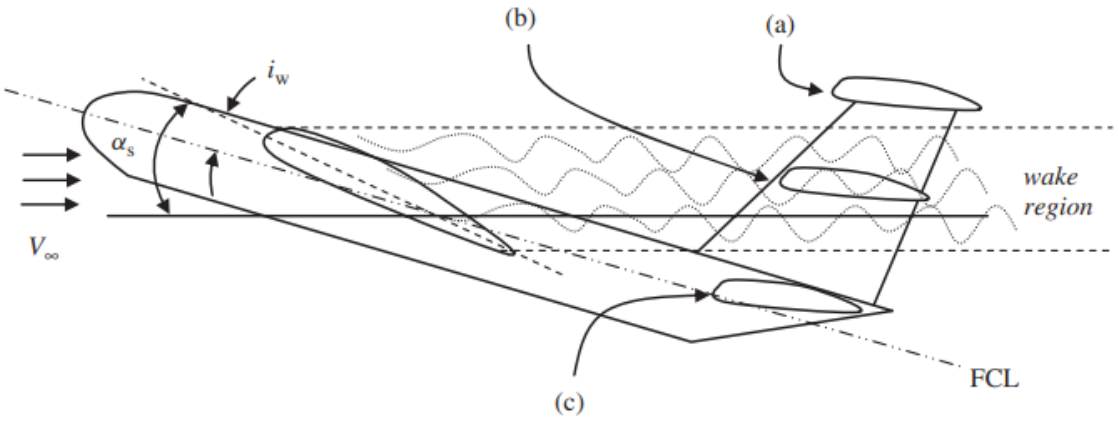

Figure 6.1: Region of wakes and downwash when aircraft is in stall condition [19]

where ht is the vertical location from FRL, α_s is the wing stall angle, i_w is the wing incidence angle.

Though high tail (T-tail) looks like the best possible option as it is completely free from wakes and downwash, The dangerous situation of deep stall can affect it severely, So when the angle of attack goes far above than the original stall angle, it faces severe pitching moment instabilities. So, considering all this, at the preliminary stage we have decided to go with conventional tail type where the horizontal tail is mounted on the fuselage and would like to consider and explore other tail types for future missions.

6.1 Horizontal Tail

The horizontal tail also called the horizontal stabilizer is solely responsible for longitudinal stability, trim and control.

6.1.1 Optimum tail arm

The tail arm is one of the most important parameter to determine in designing tails. Two basic tail parameters which interact most are the tail arm and tail area. The latter is responsible for generation of the tail lift. As the tail arm is increased, the tail area must be decreased, while as the tail arm is reduced, the tail area must be increased. So we need to find the optimum tail arm

which can be found as follows:

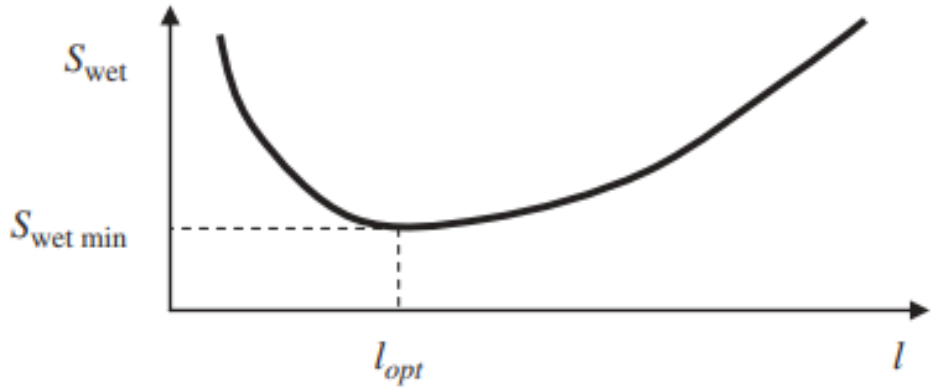

Figure 6.2: The variation of wetted area with respect to tail arm [19]

$$l_{opt} = K_c \sqrt{\frac{4\bar{C}S\bar{V}_H}{\pi D_f}} \tag{6.3}$$

where K_c is a correction factor, $\bar{C}$ is the mean aerodynamic chord of the wing. S is the surface area of the wing, $\bar{V}_H$ is volume coefficient, D_f is the maximum fuselage diameter. By substituting the values we get the optimum tail arm as

$$l_{opt} = 1.4704m \tag{6.4}$$

6.1.2 Airfoil Section

The important thing to consider while selecting airfoil is that the tailplane lift curve slope should be as high possible and it should be able to produce both positive and negative lift. This requirement necessitates the tailplane behaving similarly in both positive and negative angles of attack. For this reason, a symmetric airfoil section is a suitable candidate for a horizontal tail. NACA 0009 and NACA 0014 are the most commonly used airfoils for tails. based on requirements, we have chosen NACA 0009 as our airfoil for both horizontal and vertical tail.

6.1.3 Tail incidence, Tail setting angle

The tail setting angle can be obtained from the following equation[19]:

$$\alpha_h = \alpha_{aircraft} + i_h - \epsilon \tag{6.5}$$

where α_h is the tail incidence angle, $\alpha_{aircraft}$ is the angle of attack for aircraft will be zero in normal cruise condition as we are considering level flight, i_h is the Tail setting angle, and ϵ is the downwash.

$$i_h = \alpha_h + \epsilon \tag{6.6}$$

Now α_h can be found from the following expression:
Our design CL is 0. The pitching moment coefficient of wing plus fuselage combination 'C_{mowf} ' at wing aerodynamic center can be given as

$$C_{mowf} = C_{maf}\frac{AR cos^2\Lambda}{AR + 2cos\Lambda} + 0.01\alpha_t$$

where AR is aspect ratio, Λ is sweep and α_t is wing twist

$$C_{mowf} = -0.155\frac{11cos^2(0)}{11 + 2cos(0)} + 0.01 * (0) = -0.1312$$

The pitching moment trim equation about CG of UAV is given by

$$C_{mowf} + CL\frac{(X_{CG} - X_{ACw})}{\bar{C}} - \eta_h\bar{V}_h C_{Lh} = 0 \tag{6.7}$$

Where $\frac{(X_{CG} - X_{ACw})}{\bar{C}}$ is the static margin of UAV, which is generally 0.1 to 0.3 for most of UAVs. For preliminary analysis, the static margin is taken as 0.2. η_h is horizontal tail efficiency and it varies from 0.85-0.95. we have taken it as 0.85 which is the case for most of the UAVs.
Solving the above equation we get the value of the CL as

$$C_{Lh} = 0.0374 \tag{6.8}$$

Now The tail incidence angle can be calculated as,

$$\alpha_h = \frac{C_{Lh}}{C_{L\alpha h}} \tag{6.9}$$

where, $C_{L\alpha h}$ is the lift curve slope of the horizontal tail. It is different from C_{lh}, as $C_{l\alpha h}$ doesn't include the three dimensional effects of the tail.

$$C_{l\alpha h} = 0.1108 deg^{-1} = 6.3484 rad^{-1} \tag{6.10}$$

$$C_{L\alpha h} = \frac{C_{l\alpha h}}{1 + \frac{C_{l\alpha h}}{\pi . AR_h}} \tag{6.11}$$

$$C_{L\alpha h} = 0.0868 deg^{-1} = 4.977 rad^{-1} \tag{6.12}$$

Therefore The tail incidence angle

$$\alpha_h = 0.4297 deg \tag{6.13}$$

The downwash can be calculated as follows:

$$\epsilon = \epsilon_0 + \frac{\partial \epsilon}{\partial \alpha} \alpha_w \tag{6.14}$$

where ϵ_0 (downwash angle at zero angle of attack) and $\frac{\partial \epsilon}{\partial \alpha}$ (downwash slope) are found as follows:

$$\epsilon_0 = \frac{2 C_{Lw}}{\pi . AR} = 0.0426 \tag{6.15}$$

$$\frac{\partial \epsilon}{\partial \alpha} = \frac{2 C_{L\alpha_w}}{\pi . AR} = 0.0072 deg^{-1} = 0.4125 rad^{-1} \tag{6.16}$$

As discussed in the previous chapter, the wing incidence (α_w) for our UAV is 0.5148 deg.
Therefore the downwash is

$$\epsilon = 0.0426 + (0.0072 deg^{-1}) * 0.5148 deg \tag{6.17}$$

$$\epsilon = 0.0614 \tag{6.18}$$

from 6.6 The Tail setting angle will then be given as

$$i_h = 0.4297 + 0.0615 = 0.4912deg \tag{6.19}$$

6.1.4 Aspect Ratio

Aspect ratio is the ratio of the span to the mean aerodynamic Chord. The tail Aspect ratio tends to have direct effect on the tail lift-curve slope. As the tail aspect ratio is increased, the tail lift curve slope is increased. The initial value of the aspect ratio can be determined as follows

$$AR_h = \frac{2}{3} AR_w \tag{6.20}$$

$$AR_h = \frac{2}{3} * 11 = 7.3333m^2 \tag{6.21}$$

The final value for the tail aspect ratio will be determined based on the aircraft stability and control, cost, and performance analysis evaluations after the other aircraft components have been designed.

6.1.5 Taper Ratio, sweep, and Dihedral Angle

For the preliminary design the Taper ratio is taken to be 1, The sweep and the dihedral angle are taken to be the same as that of the wing which is zero. The final value for these parameters will be determined based on the aircraft stability and control, cost, and performance analysis evaluations after the other aircraft components have been designed.

6.1.6 other tail parameters

The span of the vertical tail can be obtained as follows

$$b_h = \sqrt{AR_h.S_h} \tag{6.22}$$

The chord length can be obtained as

$$\bar{C}_h = \frac{b_h}{AR_h} \tag{6.23}$$

substituting the values we get the span and chord length for the horizontal tail as

$$b_h = 1.1416m \tag{6.24}$$

$$\bar{C_h} = 0.1557m \tag{6.25}$$

If there is any taper ratio other than 1, the root and tip chord length can be calulated from below equations.

$$\bar{C_h} = \frac{2}{3} C_{hroot} (\frac{1 + \Lambda_h + \Lambda_h^2}{1 + \Lambda_h}) \tag{6.26}$$

$$C_{htip} = \Lambda_h C_{hroot} \tag{6.27}$$

6.2 Vertical Tail design

Vertical tail also called as vertical stabilizer is responsible directional stability of the aircraft. It is also responsible for directional trim and control.

6.2.1 Vertical tail moment arm

The vertical moment arm plays very important when dealing with a phenomena called spin, similar to how stall is. for the horizontal tail. Increasing the vertical tail moment arm increases the values of the derivatives C_{n_β} and C_{n_r} and thus makes the aircraft directionally more stable.

An increase in the vertical tail moment arm improves the directional and lateral control. In the early stage of the vertical tail design, where other aircraft components have not been designed, the vertical tail moment arm is selected to be equal to the horizontal tail moment arm. This assumption means that the vertical tail is located at the same distance from the wing as the horizontal tail. The assumption will be modified in the later design stage, when the aircraft directional and lateral stability, control, and trim are analyzed.

$$l_v = l_h = l_{opt} = 1.4704m \tag{6.28}$$

6.2.2 Volume coefficient

Volume coefficient is another very important parameter responsible for stability. For home-built UAVs, the typical value of volume flow coefficient is about 0.04.

6.2.3 Planform area

Planform area is another important parameter in determining the longitudinal stability as it is directly proportional. The planform area must be large enough to satisfy the stability, trim and control requirements. But again increase in the area means increase in the weight. Therefore we need to chose the optimum. The vertical tail area is determined as

$$S_v = \frac{b.S.\bar{V}_v}{l_v} \tag{6.29}$$

Where l_v = Vertical tail moment arm, b and S are the span and Area of the wing. Substituting the values we get the planform area as

$$S_v = 0.1923m^2 \tag{6.30}$$

6.2.4 Aspect Ratio

Typical Aspect ratios for vertical tail are 1.0-2.0. At the preliminary stage, we take aspect ratio to be 1.5. The parameter will be modified as per the requirements after doing the other parameters selection and the stability, trim and control analysis.

6.2.5 Taper ratio

The Taper ratio is the ratio of the tip chord length to root chord length. It reduces the bending stress on the vertical tail root and allow the vertical tail to have sweep angle. But apart from that it increases the complexity to manufacturing of the tail and also increases the weight. Typical values for an UAV are around 0.4-0.6. At the preliminary stage we take it to be 1 meaning both the root chord and tip chord are same and equal to mean aerodynamic chord.

6.2.6 Other vertical Tail Parameters

These parameters can be obtained in a similar way to how we obtained for horizontal tail The Span of the vertical tail can be obtained as

$$b_v = sqrt(AR_v.S_v) \tag{6.31}$$

The Chord length can be obtained as

$$\bar{C_v} = \frac{b_v}{AR_v} \tag{6.32}$$

After substituting the values, the span and the chord of the vertical tail are as follows:

$$b_v = 0.5470m \tag{6.33}$$

$$\bar{C_v} = 0.3580m \tag{6.34}$$

Now if we plan to have a taper ratio(Λ_v) other than 1, the root chord and tip chord can be obtained from the following expressions:

$$\bar{C_v} = \frac{2}{3} C_{vroot} (\frac{1 + \Lambda_v + \Lambda_v^2}{1 + \Lambda_v}) \tag{6.35}$$

$$C_{vtip} = \Lambda_v . C_{vroot} \tag{6.36}$$

The Tail design/sizing similar to wing design is an iterative process. The parameters chosen are for preliminary analysis. These are not sufficient. The design needs to go through several iterations which includes stability checks, updating the parameters, etc so as to get the best possible design.

Chapter 7

Motor Selection

Two kinds of motors are employed in the UAV, one to drive the propeller blades while the other to drive the rotor blades. We have already calculated the Power required during each phase of the mission segment. Propellers are being used during cruise, while rotors are used during take off, landing and hover. We have considered the highest power the motor needs to operate at, during its entire course. The power requirement Data is as follows: Considering motor efficiency to be 0.85, we have the power requirements as

Name of the segment	time(s)	Power(W)	Energy(KJ)
take off	90	13358	1202.2
transition	30	18.8408	564.1438
cruise (Forward)	1800	150.4383	270.79
loiter	300	150.4383	45.132
Hover	30	5109.7	153.29
cruise (Return)	1800	150.4383	270.79
transition	30	18.8408	564.1438
Landing	60	9509.8	570.59

$$P_{max}(Rotor) = 15715W$$

$$P_{max}(Propeller) = 176.986W$$

7.1 Rotor Motor

We are using four rotors to provide the necessary thrust. To find the necessary dimensions of rotor blades, loading capacity of Motors at 4000W for various blade profiles is checked. This comparison data is provided by the

manufacturer, and after careful consideration following motor and rotor blade profiles are chosen.

Throttle	Current(A)	Power(W)	Thrust(G)	RPM	Efficiency	OperatingTemperature
50	9	360	4536	1608	12.60	77.5
55	11.5	460	5240	1769	11.39	77.5
60	14.6	584	6320	1907	10.82	77.5
65	17.6	704	7284	2041	10.35	77.5
75	25.1	1004	8805	2306	8.77	77.5
85	33.5	1340	10969	2529	8.19	77.5
100	51.6	2064	14421	2872	6.99	77.5

According to the manufacturer, above data represents the rotor performance with a 34 cm long rotor blade. The motor with this configuration of rotor blades is capable of lifting around 11 Kgs of weight. So, four individual rotors with individual motors are considered. The rotor profile includes, four blades which are 34 cm long.

The Motor selected is TIGER MOTOR U POWER U13 85KV, Model:**RKI-3794**. The Motor Parameters are as follows: Motor Specifications are:

Figure 7.1: RKI-3794

Internal Resistance = 18mΩ
Configuration = 18N24P
Motor Dimensions = 118.4/56.8 mm
Weight including cables = 1300 g
Max continuous Power 180S = 3848 W

7.2 Propeller Motor

$$P_{max}(Propeller) = 176.986W$$

Similarly, T-motor **MN5212 KV340** brushless motor is chosen, its standard performance and design specifications mentioned by the manufacturer are shown below.

Throttle	Current(A)	Power(W)	Thrust(G)	RPM	Efficiency	Torque
50	6.8	162.2	1204	4976	7.42	0.321
55	8.7	208.1	1478	5487	7.10	0.278
60	10.5	302.2	1746	5947	6.94	0.33
65	12.6	405.6	1983	6376	6.56	0.374
75	18.8	599	2589	7287	5.75	0.493
85	25	720.1	3230	8042	5.39	0.607
100	36.7	881.3	4175	9091	4.74	0.784

From the above table it can be seen that with a 15 x 5 CF propeller combination the required parameters are obtained at their corresponding throttle input.

Figure 7.2: MN5212 KV340 Brushless motor

Motor dimensions:	$\phi 59 \times 33.25$mm
Stator diameter:	52mm
Stator height:	12mm
Shaft diameter:	4mm
Weight including cables:	249g

Table 7.1: Specifications of MN5212 KV340

Figure 7.3: 15 x 5 Propeller

Weight:	13g
Diameter:	15inch(381.1mm)
Pitch:	5inch(127mm)
Material:	CF + Epoxy

Table 7.2: Specifications of propeller

Chapter 8

CAD Model

Considering the deduced dimensions of the Wing, Tail, Rotors and Fuselage, we designed the UAV in Fusion 360. The model looks as follows:

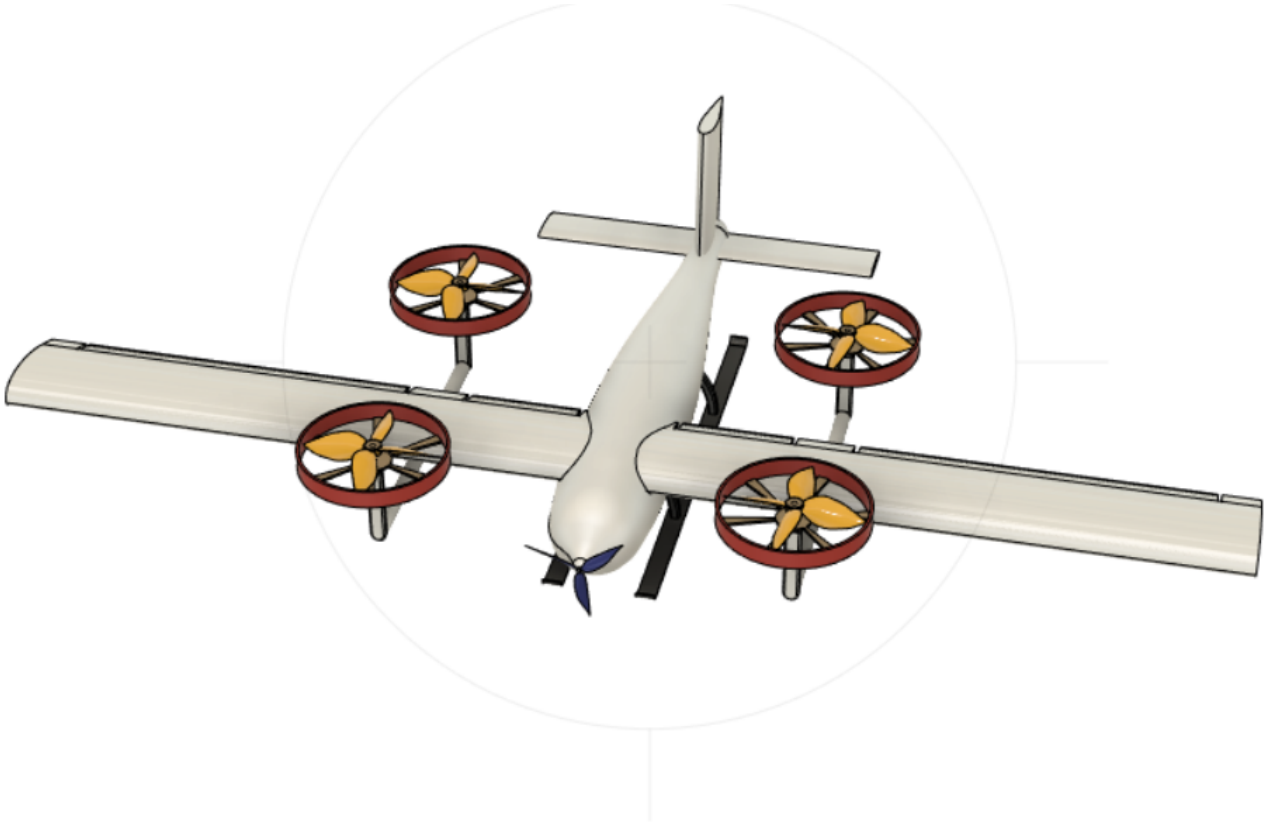

Figure 8.1: CAD Model of the UAV

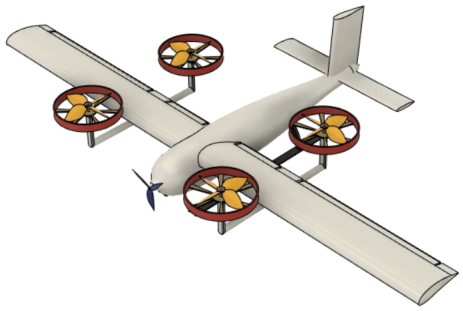

(a) Oblique view

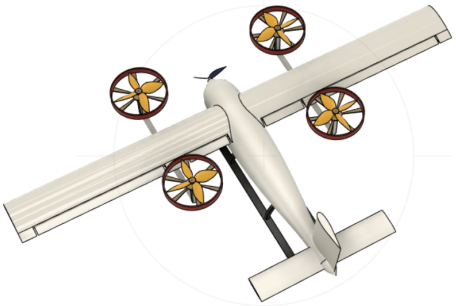

(b) UAV

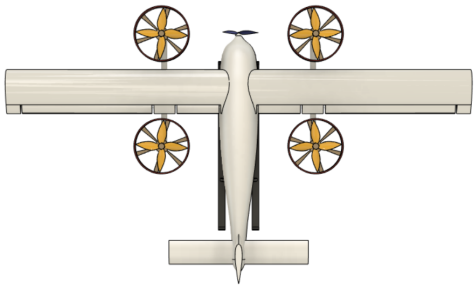

(c) Top view

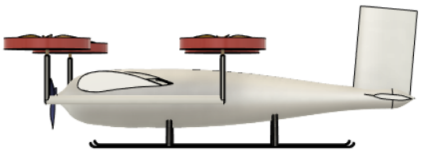

(d) Right view

(e) Front view

(f) UAV

Figure 8.2: CAD Model of UAV

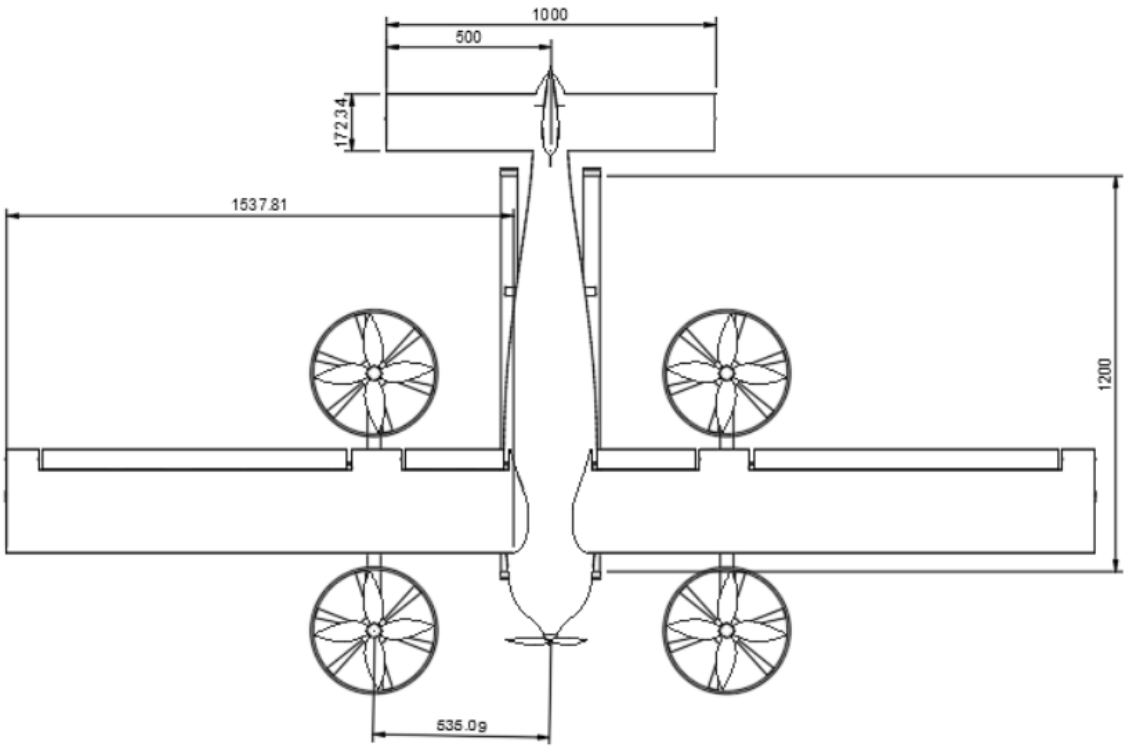

Figure 8.3: Projected view(All dimensions in mm)

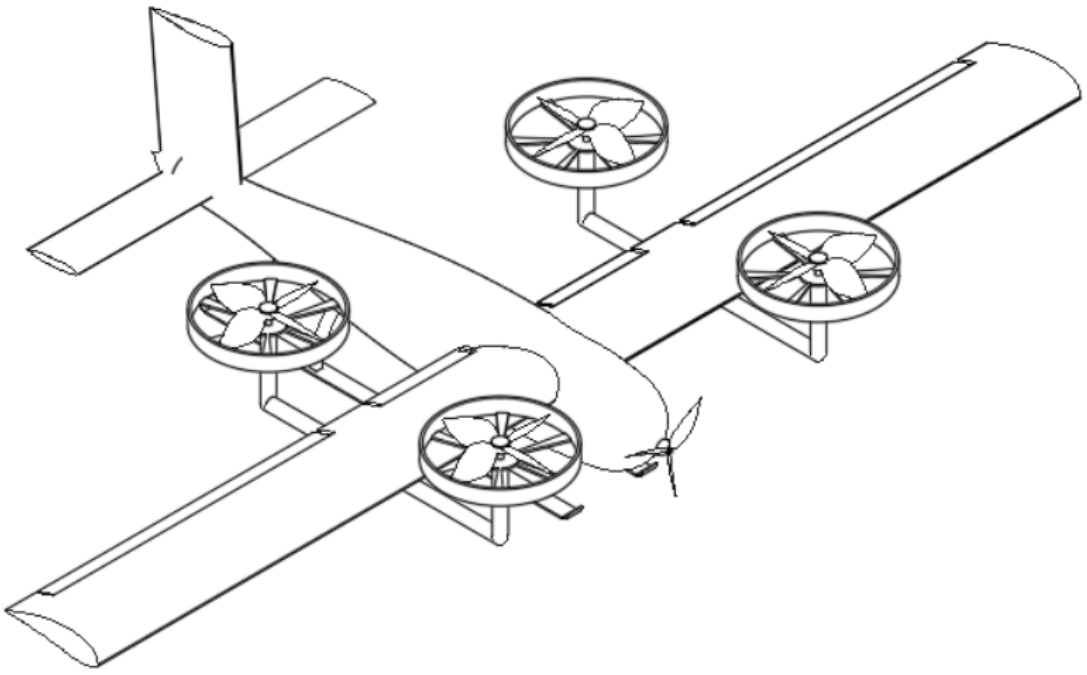

Figure 8.4: Isometric projected view

Chapter 9

Component Placement and CG Calculation

The payload bay, batteries, forward motor and avionics will be placed in the fuselage in the following manner:

The forward motor is placed at the nose. Behind this, the batteries are placed, followed by the avionics bay (sensors, etc.), and then the payload bay. The payload box will be inside the UAV, and released on landing using a solenoid latch mechanism. The ESCs for all the motors are placed towards the tail.

9.1 CG calculation

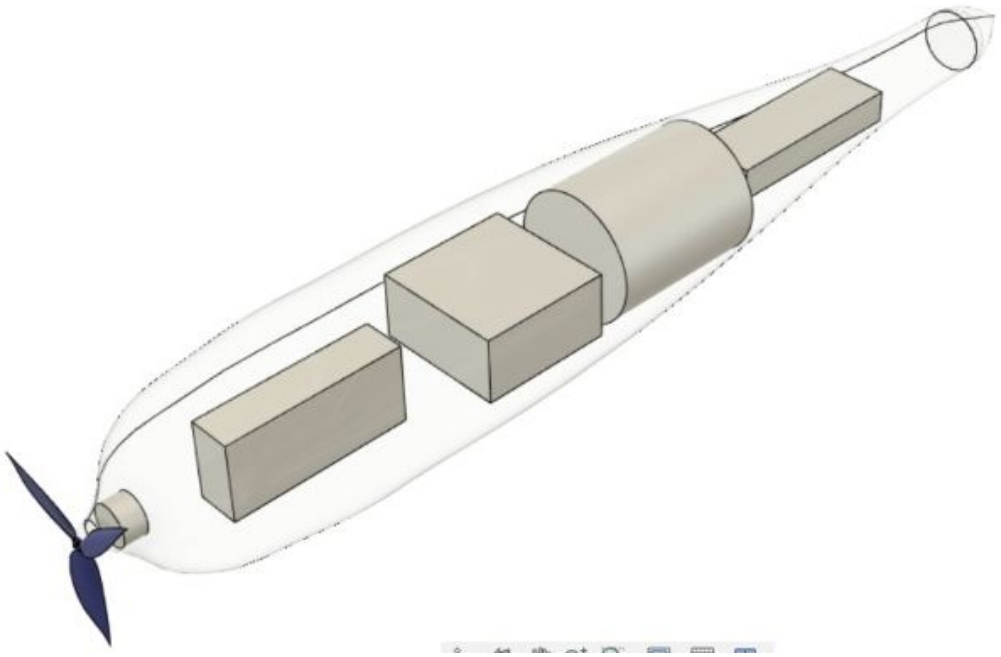

Figure 9.1: Internal Component Placement

Chapter 10

Performance Analysis

10.1 Drag estimation

[22] The drag polar can be written as:

$$C_D = C_{D_0} + KC_L^2$$

Here,

$$C_{D_0} = (C_{D_0})_{WB} + (C_{D_0})_h + (C_{D_0})_v$$

At low subsonic Mach number, $(C_{D_0})_{WB}$ is given by the following equations,

$$(C_{D_0})_{WB} = C_{fw}[1 + L\frac{t}{c} + 100(\frac{t}{c})^4]R_{LS}\frac{(S_{wet})_e}{S_{ref}} +$$

$$+C_{fb}[1 + \frac{60}{(I_B/d)^3} + 0.0025\frac{l_B}{d}]\frac{(S_S)_e}{S_{ref}}R_{WB} + C_{Db}\frac{S_B}{S_{ref}}$$

where,
S_{ref} = Wing Planform Area = $1.109m^2$
$(S_{wet})_e$ = wetted area of wing = 2^*S_{ref}
$(S_S)_e$ = exposed wetted area of the body = 2.218 m^2
S_B = Body minimal frontal area = $\pi * 0.28^2/4$
$\frac{I_B}{d}$ = body fitness ratio = $\frac{1.193}{0.15}$ = 7.953 C_{fw} = turbulent flat plate skin coefficient of the wing including roughness effects, as a function of Reynolds number and Mach number based on mean aerodynamic chord of wing = 0.00612
C_{fB} = turbulent flat plate skin coefficient of the body including roughness effects, as a function of Reynolds number and Mach number based on actual;

body length $l_B = 0.0038$
L = 2 for $(t/c)_{max}$ $\frac{t}{c}$ = average streamwise thickness ratio of wing = 0.1
R_{LS} = Lifting surface correction factor = 1.08
R_{WB} = Wing-body interference correlation factor = 1.08
C_{Db} = base drag coefficient based on maximum body frontal area given as:

$$C_{Db} = \frac{0.029(\frac{d_b}{d})^3}{\sqrt{(C_{Df})_b}}$$

where, d_b/d = ratio of base diameter to maximum diameter = 0.2667
$(C_{Df})_b$ = zero lift drag of body base given as:

$$(C_{Df})_b = C_{fB}[1 + \frac{60}{(l_B/d)^3} + 0.0025\frac{l_B}{d}]\frac{(S_S)_e}{S_B} = 0.1083$$

From above values,
$(C_{D_0})_{WB} = 0.0211$

10.2 Estimation of $(C_{D_0})_H$

$C_{D_{0_H}}$ is found using the formula:

$$C_{D_{0_H}} = C_{f_H}[1 + L\frac{t}{c} + 100(\frac{t}{c})^4]_p(R_{LS})_H\frac{S_{wet,H}}{S}$$

Here,
$C_{f_H} = 0.0043$
Wetted area of horizontal tail, $S_{wet,H} = 2 * 0.1777111$
$(R_{LS})_H = 1.08$
$L = 2$
$\frac{t}{c} = 0.09$
From above values,
$(C_{D_0})_H = 0.0013$

10.3 Estimation of $(C_{D_0})_V$

The $(C_{D_0})_V$ is given as,

$$(C_{D_0})_V = C_{fV}[1 + L\frac{t}{c} + 100(\frac{t}{c})^4]_p(R_{LS})_V\frac{(S_{wet})_e}{S_{ref}}$$

where,
$(S_{wet})_e$ = wetted area of vertical tail = 2*0.1922877 m^2
$C_{fV} = 0.0038$
$(R_{LS})_V = 1.08$
L = 2
$\frac{t}{c} = 0.09$

$$(C_{D_0})_v = 0.0012$$

Therfore,

C_{D_0} = 0.0211 + 0.0013 + 0.0012 + 5% interferance drag + 10% due to roughness and perturbations = 0.0271

10.4 Estimation of K

K is given as,

$$K = \frac{1}{\pi ARe}$$

The factor e can be computed as,

$$\frac{1}{e} = \frac{1}{e_{wing}} + \frac{1}{e_{fuselage}} + \frac{1}{e_{other}}$$

where,
$e_{wing} = 0.685$
$e_{fuselage}$ is given as,

$$\frac{1}{e_{fuselage}}\frac{S}{S_{fuselage}} = 2.02$$

$$\frac{1}{e_{fuselage}} = 1.3588$$

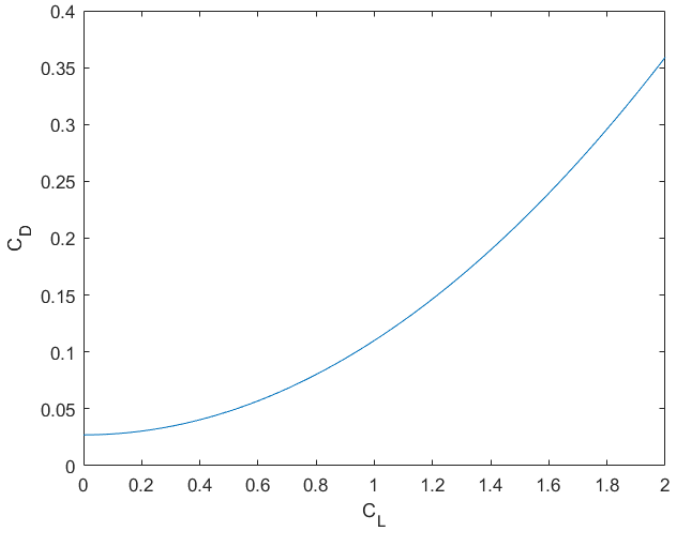

Figure 10.1: Drag Polar

$\frac{1}{e_{other}} = 0.05$ for preliminary calculations
Therefore,

$$e = 0.3486$$

$$K = 0.083$$

The drag polar can now be estimated as:

$$C_D = C_{D_0} + KC_L^2 = 0.0271 + 0.083C_L^2$$

A plot of this drag polar is shown in Figure 10.1

10.5 V-n diagram

The V-n diagram is the most important flight envelope involved in preliminary design. It helps in visualising the loads on the aircraft and determines the limits on maneuvering based on the maximum loads the aircraft. The critical points of the diagram are calculated as below:

The load factor n is defined as:

$$n = \frac{L}{W} = \frac{\rho S V^2 C_{L_{max}}}{2W}$$

Maneuver at speeds dictated by the above equation, until the limit load n_{max} is reached. $n_{max} = 3$ for a non aerobatic aircraft. The velocity corresponding to this condition is V_B. To estimate this, the 3D wing maximum lift coefficient is calculated from the 2D airfoil maximum lift coefficient using the approximation [19]:

$$C_{L_{max}} = C_{l_{max}} \times 0.95 \times 0.9$$

Similarly for the negative $C_{l_{max}}$ also we calculate the corresponding velocity $V_{B_{neg}}$. The maximum design cruise speed V_C for semiaerobatic aircraft can be calculated as:

$$V_C = V_B + 22.22$$

This speed is defined to stay within safe limits and avoid permanent structural deformation. We can also define a never cross speed or dive speed as:

$$V_D = 1.25 \times V_C$$

If we cross this speed, structural deformation is inevitable. The area between V_C and V_D is camfered to avoid excessive loads due to velocity changes that may damage the aircraft. The camfer is usually taken to be till $n_2 = 0.75 n_{max}$ and $n_3 = 0$. The negative n side of the graph is drawn similarly. The diagram is shown in Figure 10.2

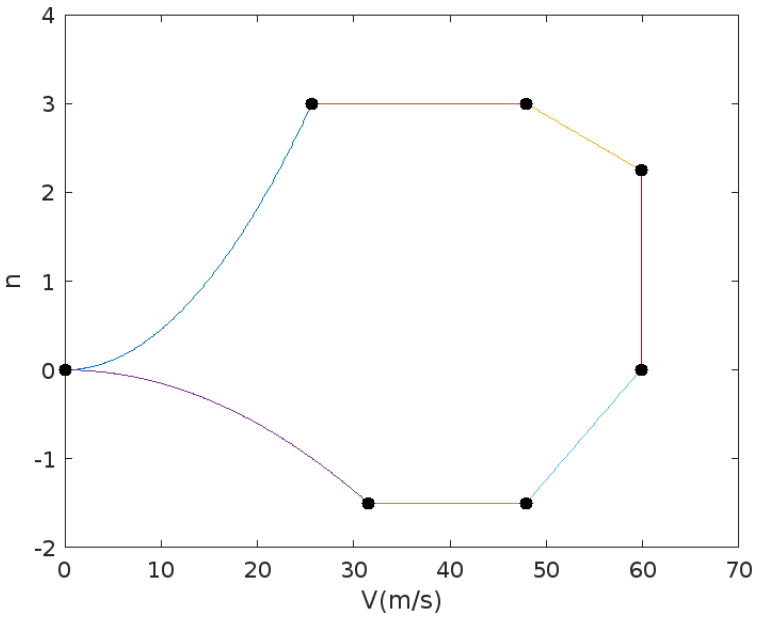

Figure 10.2: V-n diagram

Chapter 11

Static Stability Check

Stability is defined as the tendency of an aircraft to oppose a disturbance and return to its initial steady-state trim condition if disturbed.

We have two kinds of stability:

- Static stability
- Dynamic stability

Static stability is defined as the initial tendency of an aircraft to naturally attain forces and/or moments which oppose an instantaneous perturbation of a motion variable from a steady-state flight condition.

Dynamic stability is defined as the tendency of an aircraft to naturally return to the initial steady-state trim condition after any disturbance alters the trim values. Dynamic stability concerns the entire history of the motion, in particular the rate at which the motion damps out.

About the three axes of the aircraft we have three kinds of stability:

- Longitudinal stability
- Lateral or Directional Stability

11.1 Longitudinal Static stability

For an aircraft to have static longitudinal stability, pitch moment curve($C_{m,CG}$ vs. α curve) must have negative slope. i.e., $\frac{\partial C_{m,CG}}{\partial \alpha} < 0$

The contribution of wing to C_m is

$$C_{m,CG_w} = C_{L_w}\left(\frac{X_{CG} - X_{ac}}{\bar{c}}\right) + C_{m,ac_w}$$

Thus, the pitch moment curve slope due to wing is:

$$\frac{\partial C_{m,CG_w}}{\partial \alpha} = \frac{\partial C_{L_w}}{\partial \alpha}\left(\frac{X_{CG} - X_{ac}}{\bar{c}}\right) \tag{11.1}$$

as C_{m,ac_w}(pitch moment coefficient about aerodynamic center) is independent of angle of attack. The contribution of tail to C_m is:

$$C_{m,CG_t} = C_{m0,t} + \frac{\partial C_{m,CG_t}}{\partial \alpha}\alpha$$

where:

$$C_{m0,t} = \eta V_H C_{L_\alpha,t}(\epsilon_0 - i_t)$$
$$\frac{\partial C_{m,CG_t}}{\partial \alpha} = -\eta V_H C_{L_\alpha,t}\left(1 - \frac{\partial \epsilon}{\partial \alpha}\right)$$

η is tail efficiency factor due to fuselage wakes, $V_H = \frac{l_t S_t}{S\bar{c}}$ is the horizontal tail volume ratio, l_t is distance between tail and CG, S_t is the horizontal tail area, $\epsilon = \epsilon_0 + \frac{\partial \epsilon}{\partial \alpha}\alpha$ is the downwash angle due to induced velocity of the wing, $C_{L_\alpha,t}$ is tail lift curve slope and i_t is tail incidence angle.

The typical value of the η for an aircraft with a conventional tail varies from 0.85 to 0.95.[19]. For this design we choose $\eta = 0.9$.

For an elliptic wing, $\epsilon = \frac{2C_{L_w}}{\pi AR_w}$. For non-elliptic wings, there is no emperical estimate for ϵ. Thus, as an approximation we can say that

$$\frac{\partial \epsilon}{\partial \alpha} \approx \frac{2}{\pi AR_w}\frac{\partial C_{L_w}}{\partial \alpha}$$

On substituting the values we get, $\frac{\partial C_{m,CG_w}}{\partial \alpha} =$ and $\frac{\partial C_{m,CG_t}}{\partial \alpha} =$. Thus, overall pitch moment curve slope is

$$\frac{\partial C_{m,CG}}{\partial \alpha} = \frac{\partial C_{m,CG_w}}{\partial \alpha} + \frac{\partial C_{m,CG_t}}{\partial \alpha} =$$

$$\frac{\partial C_{m,CG}}{\partial \alpha} =< 0 \tag{11.2}$$

This implies that the UAV has longitudinal static stability. We note here that contribution of fuselage to C_m is not considered here. The value is usually small positive or negative values.

11.1.1 Calculation of Stick Fixed Neutral Point

Neutral Point of an aircraft is the point about which the aerodynamic pitching moment is independent of angle of attack α i.e., $\frac{\partial C_{m,NP}}{\partial \alpha} = 0$. The neutral point location is given by the expression:

$$\frac{X_{NP}}{\bar{c}} = \frac{X_{ac}}{\bar{c}} + \eta V_H \frac{\frac{\partial C_{L,t}}{\partial \alpha}}{\frac{\partial C_{L,w}}{\partial \alpha}} \left(1 - \frac{\partial \epsilon}{\partial \alpha}\right) \tag{11.3}$$

Appendix A

Reference Aircraft

After defining our mission statement and profile, we did some research on case studies with other UAV's who have similar missions and collected the relevant data from them for estimating our weight.

The case studies were done on the following,

1. EOS C - EOS C_Link
2. Yangda FW - Yangda_FW_Link
3. Yangda Sky Whale - Yangda_Sky_Whale_Link
4. Google Wing - Google_Wing_Link
5. Avy Area - Avy_Area_Link
6. Avy New Area - Avy_New_Area_Link

The data we collected from the above air craft are as follows,

SNo.	Name	MTOW(kg)	W_{pay}(kg)	W_{af}(kg)	W_b(kg)	Endurance(min)	Range(km)
1	EOS C	14.4	1.1	11	2.3	120	180
2	Yangda FW-320	23	5	9.76	7.2	150	-
3	Yangda Sky Whale	34	10	16	7.2	60	100
4	Google Wing	6.4	1.2	2.74	2.46	-	20
5	Avy Area	12	1.5	6.89	3.61	55	60
6	Avy new Area	19.5	3	7.5	9	60	80

Appendix B

Battery Energy estimation

The MATLAB code used to estimate energy of the battery is given below.

```
clc; clear; close all;
%%
AR = 9.2;
Aprop=pi*(25.4e-2)^2/4;%10 inch
b=2; Vcruise=90*5/18;
CL=0.47;
Taperratio=0.78;
twist=-1;
clmax = 1.318;
CD0=0.0447;
S = 0.485;
e = 0.778;
K = pi*AR*e;
K = 1/K;
CD = CD0+K*CL^2;%e=0.778
Wo = 20*9.81;%guess value
Wpayload=5*9.81;
K_T = 1.2;
[¬,¬,¬, rho_g] = atmosisa(5e+03);
[¬,¬,¬,rho_cruise] = atmosisa(5.1e+03);
%%
%take-off
V_TO = 100/90;
W_TO = Wo;
T_TO = K_T*W_TO;
P_TO= T_TO*V_TO/2*(1+sqrt(1+2*T_TO/(rho_g*V_TO^2*Aprop)))
E_TO = P_TO*90
%%
%transition(takeoff->cruise)
%P_Trans1 = Wo*Vcruise
P_Trans1 = 0.5*rho_cruise*S*CD*(Vcruise/2)^3
E_Trans1 = P_Trans1*30
%%
%cruise1
P_cruise1 = 0.5*rho_cruise*S*CD*Vcruise^3
E_cruise1 = P_cruise1*1800
%%
%loiter(same as cruise)
P_loiter = P_cruise1
E_loiter = P_loiter*300
%%
```

```
%cruise2(return)
P_cruise2 = P_cruise1
E_cruise2 = E_cruise1
%%
%transition(cruise->landing)
W = Wo-Wpayload;
% P_Trans2 = W*Vcruise
P_Trans2 = 0.5*rho_cruise*S*CD*(Vcruise/2)^3
E_Trans2 = P_Trans2*30
%%
%landing
VH = sqrt(W/(2*rho_g*Aprop));
Vi = @(x) ((1.2-1.25*x-1.372*x^2-1.718*x^3-0.655*x^4)*VH);
Vdescent = 4;
Vi  = Vi(-Vdescent/VH);
P_Landing = 1.2*W*(Vi-Vdescent)
E_Landing = P_Landing*60
%%
T = Wo/4;
A=pi*(25.4e-2)^2/4;%10 inch
FoM = 0.7;
P_Hover = T/FoM*sqrt(T/(2*rho_cruise*A))*4
E_Hover = P_Hover*30
%%
E = E_TO+E_Trans1+E_cruise1+E_loiter+...
    E_cruise2+E_Trans2+E_Landing+E_Hover%in J
E = E/3600%in Watt-hour
```

Appendix C

First weight estimation(MTOW)

The below MATLAB code shows the MTOW estimate given battery weight estimate and empty weight fraction-total weight emperical relation.

```
clc; clear; close all;
%all mass in kg
Wb=2.604*3;%3 LiPo 22.2V Orange 22000mAh batteries
A=0.5963;
C=-0.0582;
Wo_initial = 20;
We_by_Wo = A*Wo_initial^C;
Wpayload =5;
Wo_array = Wo_initial;
Wo =Wo_initial;
for i = 1:20
  Wo =  (Wpayload+Wb)/(1-A*Wo^C);
  Wo_array = [Wo_array;Wo];
end
plot(0:i, Wo_array,'Marker','*','LineWidth',2);
set(gca,'FontSize',16);
yline(Wo_array(end),'--',"Wo|_{final}="+Wo_array(end),"Color",'m','FontSize',16)
xlabel("Iterations");
ylabel("Maximum Takeoff Weight MTOW W_0");
title("Convergence Plot");
W_final = Wo_array(end)*1.05
```

Appendix D

Wing Loading,Power Loading, Disc Loading

MATLAB code for Wing loading and Power loading part

```
clc; clear; close all;

Sh = 0.07;
Sv = 0.055;
S = 0.485;
Swet = 0.821;
AR = 9.2;
e = 0.778;
b = 2;
W = 26.5893*9.81;
CL = 0.47;
Vcruise = 25;
Clmax = 1.318;
Cd0 = 0.0447;
c = 0.2425;
nu = 1.789*10^-5;
rho = 0.7282;
h = 100; %takeoff altitude from base camp
t_to = 90; %takeoff time
[¬, ¬, ¬, rho0] = atmosisa(0);
% Vstall = sqrt(2*W / (rho*S*Clmax));
Vstall = 0.75 * Vcruise; %Veerman et al. 15% less than minimum cruise speed
Re = rho * Vcruise * c / nu;
Cfe = (2*log10(Re)-0.65)^(-2.3);
Kt = 1 + Sv/S + Sh/S;
q = 0.5 * rho * Vcruise * Vcruise;
K = 1/(pi * AR * e);
F1 = Kt*Cfe*Swet/S;
F2 = (Cd0-F1) / (W / S);
F3 = K/(q * q);

%% wing loading based on cruise

W_S =W/ S;   %Wing loading
p = q*sqrt(F1*pi*AR*e); %at t min
t_min = Vcruise.*q*((2*F1/p)+F2);
t =t_min*1.05; %5 percent tolerance
p=30:0.1:500;
```

```
y1=@(x) (Vcruise.*q*((F1./x)+F2+(F3.*x)));
y2=p-p+t;
y3=p-p+t_min;

%plotting t/w vs w/s
figure(1);
plot(p,y1(p));
hold on;
% for 5 percent tolerance of w/s optimum
w_s_5= interp1(y1(p),p,t); %solving t with y1 we get 160.9597 and 74.7
yline(y2,'--r');
legend({});
xline(160.9597, '--m');
xline(74.7, '--m');
hold on;
[T_W_min,I] = min(y1(p));
plot(p(I),y1(p(I)),'r*');
legend({'Optimum W/S for Cruise', '5% Tolerance from Optimum W/S'});
title("P/W vs W/S Based on Cruise")
xlabel("W/S");
ylabel("P/W");



%% ROC constraint
%p = 0:2:500;
ROC = h / t_to; %rate of climb
PbyW = (@(p) (ROC + sqrt(F1 .* K) ./ F2 .* (F1 ./ p + F2 + F2^2 .* p ./ F1)));

figure(2);
plot(p, PbyW(p));
hold on;
popt = F1 / F2;
PbyWopt = ROC + 3 * sqrt(F1 * K);
plot(popt, PbyWopt, '*r');
[val, ind] = min(PbyW(p));
ptolup = fsolve(@(p) (PbyW(p) - 1.05 * PbyWopt), 510);
ptoldown = fsolve(@(p) (PbyW(p) - 1.05 * PbyWopt), 24);
yline(PbyWopt * 1.05);
xline(ptolup);
xline(ptoldown);

title("P/W vs W/S Based on Rate of Climb Constraint")
xlabel("W/S");
ylabel("P/W");
legend('ROC Constraint', 'Optimum point', '5% Tolerance P/W', '5% Tolerance W/S', '5% ...
    Tolerance W/S', 'FontSize', 14);

%%
%Wing loading based on Absolute ceiling constraint
%p = 30:2:500;
Vc = 25;
Vhmax = @(p1)(4*K*p1.^2/(3*rho^2*(F1+F2.*p1))).^0.25;
Qhmax = @(p1) 0.5*rho*Vhmax(p1).^2;
t_hmax = (4*K*(F1+F2*p)).^0.5; %when at max height, Treq = Dmin  condition is considered.
t_hmax_Vmax = (2*q*(F1./p+F2)); %when prescribed velocity is considered at max height.
Pw_hmax = @(p1) (Vc*(4*K*(F1+F2*p1)).^0.5); %when at max height, Treq = Dmin  condition is ...
    considered.

Pw_hmax_Vmax = @(p1) (Vhmax(p1)*(2*Qhmax(p1)*(F1./p1+F2))); %when prescribed velocity is ...
    considered at max height.

fun = @(p1) Vc*((4*K*(F1+F2*p1)).^0.5 - (2*q*(F1./p1+F2)));
p_int = fsolve(fun,10); %int:intersection
p_opt = p_int;
```

```
t_opt = (4*K*(F1+F2*p_opt)).^0.5;
Pw_opt = Vc*(4*K*(F1+F2*p_opt)).^0.5;
%for 5 percent tolerence
t_opt_max = t_opt * 1.05;
t_opt_min = t_opt * 0.95;
Pw_opt_max = Pw_opt * 1.05;
Pw_opt_min = Pw_opt * 0.95;
figure(3)
plot(p,Pw_hmax(p),p,Pw_hmax_Vmax(p),'r')
pa = ((Pw_opt_max/Vc)^2/(4*K) - F1)/F2; %corresponds to max
pb = ((Pw_opt_max/Vc)^2/(4*K) - F1)/F2;
pc = F1/(Pw_opt_max/(2*q*Vc) - F2);
pd = F1/(Pw_opt_min/(2*q*Vc) - F2);
xline(p_opt, '--b')
yline(Pw_opt_max, '--k')
xline(pa, '--g');
xline(pc, '--m');
xline(pb, '--g');
xline(pd, '--m');
yline(Pw_opt,'g')
yline(Pw_opt_min, '--k')
legend({'P/W vs W/S for Hmax','P/W vs W/S for V at Hmax' 'Optimum point', '5% Tolerance ...
    from Optimum P/W','Tolerance on Optimum W/S w.r.t Hmax Consideration','Tolerance on ...
    Optimum W/S w.r.t V Hmax Consideration'});
xlabel("W/S")
ylabel("P/W")
title("P/W vs W/S Based on Absolute ceiling Constraint")

%% combined plot
figure(4);
hold on;
plot(p,y1(p))
plot(p, PbyW(p))
plot(p,Pw_hmax(p))
plot(p,Pw_hmax_Vmax(p))
p_vStall = 0.5*rho*Vstall*Vstall*Clmax;
xline(p_vStall, 'k');
Preq = 1138.5;
PbyWreq = Preq / W;
yline(PbyWreq, 'c');
% func = @(p1) (Pw_hmax_Vmax(p1) - y1(p1));
% p_opt_final = fsolve(func, 140);
p_index = find(abs(Pw_hmax_Vmax(p) - y1(p)) < 0.0001, 1);
p_opt_final = p(p_index);
plot(p_vStall, PbyWreq, 'r*');
%area((p(1):1:round(p_vStall, 0)), ...
    {Pw_hmax_Vmax(p(1):1:p_opt_final),y1(p_opt_final:1:round(p_vStall, 0))}, 'FaceColor', ...
    'y', 'FaceAlpha', 0.5);
xlabel('W/S');
ylabel('P/W');
legend('cruise','ROC','Hmax','V_Hmax','stall')
```

MATLAB Code for Disc Loading

```
clc; clear; close all;
%%
%hover
W = 26.5893*9.81;
T = W/4;
A=pi*(25.4e-2)^2/4;%10 inch
[¬,¬,¬, rho] = atmosisa(5e+03);
ki = 1.15;
```

```
DL = T/A
FoM = 0.7;
P = T/FoM*sqrt(DL/rho*0.5)*4
```

Appendix E

Airfoil selection

```
%% airfoil selection

clc; clear all; close all;

% reference: Mohammed Sadrey "Aircraft Design: A Systems Engg. Approach"

%step1
W = 26.5893 * 9.81;
rho = 0.7282;
[¬, ¬, ¬, rho0] = atmosisa(0);
Vc = 25;
WbyS = 168.7091;
S = W / WbyS;
Vstall = 0.75 * Vc;

%step 2: aircraft ideal cruise lift coefficient
CLC = 2 * WbyS / (rho * Vc * Vc);

%step 3: wing cruise lift coefficient
CLCw = CLC / 0.95; %approximation

%step 4: wing airfoil ideal lift coefficient
Cli = CLCw / 0.9; %approximation

%step 5: aircraft maximum lift coefficient
CLmax = 1.318;

%step 6: wing maximum lift coefficient
CLmaxw = CLmax/ 0.95; %approximation

%step 7: wing airfoil gross maximum lift coefficient (with HLD included)
Clmaxgross = CLmaxw / 0.9; %approximation

%step 8: HLD contribution
ΔClHLD = 0;

%step 9: wing airfoil net maximum lift coefficient
Clmax = Clmaxgross - ΔClHLD;
```

Appendix F

Wing Design

Appendix G

Fuselage Length

The below code explains how the fuselage length is calculated.

```
clc; clear; close all;
L = [1.2;1.92;1.3;1.8;1.5];
W0 = [23;34;6.4;14.2;19.5];
figure(1)
scatter(log(W0),log(L),"LineWidth",1.5);
hold on
p = polyfit(log(W0),log(L),1);
x1 = log(5:0.01:40);
y1 = p(1)*x1+p(2);
plot(x1,y1,"LineWidth",2)
W = 26.5893;
a = exp(p(2))
c = p(1)
Fuselage_length = a*W^c
plot(log(W),log(Fuselage_length),"k^","LineWidth",2)
set(gca,'FontSize',16);
xlabel("$\log(W_0)$", "Interpreter","latex");
ylabel("$\log$(Fuselage Length)", "Interpreter","latex");
title("Fuselage Length vs. MTOW plot($\log - \log$ scale)", "Interpreter","latex");
legend("Data Points", "Linear fit","Design Point");
```

Appendix H

Drag Estimation

```
clc; clear all; close all;

Cfw = 0.00612;
CfB = 0.0038;
L = 2;
lBd = 7.953;
Sref = 1.5461;
Swet = Sref*2;
SSe = 1.109*2;
SB = pi * 0.28 * 0.28 / 4;
tbyc = 0.04255;
RLS = 1.08;
RWB = 1.08;
dbbyd = 0.2667;
CDfb = CfB * (1 + 60 / (lBd^3) + 0.0025*lBd) * SSe / SB;
CDB = 0.029*dbbyd^3 / sqrt(CDfb);
CD0WB = Cfw * (1 + L*tbyc + 100 * tbyc^4) * RLS * Swet / Sref + CDfb * SB / Sref * RWB + ...
    CDB * SB / Sref;

L2 = 2;
tbyc2 = 0.09;
RLSH = 1.08;
CfH = 0.0043;
SwetH = 2 * 0.1777111;
CD0H = CfH * (1 + L2 * tbyc2 + 100 * tbyc^4) * RLSH * SwetH / Sref;

L3 = 2;
tbyc3 = 0.09;
RLSV = 1.08;
CfV = 0.0038;
SwetV = 2 * 0.1922877;
CD0V = CfV * (1 + L3 * tbyc3 + 100 * tbyc^4) * RLSV * SwetV / Sref;

CD0 = (CD0WB + CD0V + CD0H) * 1.15;

ewing = 0.685;
Sfus = 1.04;
byefus = 2.02 * Sfus / Sref;
byeother = 0.05;
e = 1 / (1 / ewing + byefus + byeother);

AR = 11;
K = 1 / (pi * AR * e);
```

```
43
44 CD = @(CL) (CD0 + K * CL * CL);
45 figure;
46 plot(0:0.01:2, CD(0:0.01:2));
47 xlabel('C_L');
48 ylabel('C_D');
```

Appendix I

V-n diagram

```
%% Vn diagram 2

clc; clear all; close all;

npos = 3;
nneg = -0.5*npos;

Vcr = 25;
WbyS = 168.7091;
W = 26.5893 * 9.81;
S = W / WbyS;
PbyW = 4.3647;
rho = 0.7282;
Clmax = 2.47;
Clmaxneg = -0.818;
CLmax = Clmax * 0.9 * 0.95;
CLmaxneg = Clmaxneg * 0.9 * 0.95;
CD0 = 0.0271;
K = 0.083;
Vstall = 0.75 * Vcr;
nposvals = @(V) (rho .* S .* CLmax .* V .* V ./ (2 * W));
nnegvals = @(V) (rho .* S .* V .* V .* CLmaxneg ./ (2 * W));
Vb = fsolve(@(V) (nposvals(V) - npos), 50);
Vc = Vb + 80 * 5 / 18;
% Vd = fsolve(@(V) (WbyS .* sind(30) + PbyW .* WbyS ./ V - 0.5 .* rho .* V .* V * sqrt(3 * ...
    CD0 / K)), 80);
Vd = 1.25*Vc;

n2 = 0.75 * npos;
n3 = 0;

Vbneg = fsolve(@(V) (abs(nnegvals(V)) - abs(nneg)), 30);
% Vcneg = Vbneg + 80 * 5 / 18;

rx = n2:-0.0001:n3;
ry = Vd.*ones(length(rx),1);
%plot(Vd .* ones(length(n2:0.1:n3), 1), n2:0.1:n3);
figure;
plot(0:0.1:Vb, nposvals(0:0.1:Vb));
hold on
plot(Vb:0.1:Vc, npos .* ones(length(Vb:0.1:Vc), 1))
plot(Vc:0.1:Vd, linspace(npos, n2, length(Vc:0.1:Vd)));
plot(0:0.1:Vbneg, nnegvals(0:0.1:Vbneg));
```

```
plot(Vbneg:0.1:Vc, nneg .* ones(length(Vbneg:0.1:Vc), 1));
plot(Vc:0.1:Vd, linspace(nneg, n3, length(Vc:0.1:Vd)));
plot(ry,rx);
xlim([0, 70]);
ylim([-2, 4]);
xlabel('V(m/s)');
ylabel('n');
plot([0, Vb, Vc, Vd], [0, nposvals(Vb), nposvals(Vb), n2], '.k', 'MarkerSize', 20)
plot([0, Vbneg, Vc, Vd], [0, nnegvals(Vbneg), nnegvals(Vbneg), n3], '.k', 'MarkerSize', 20)
```

Bibliography

[1] *Hybrid VTOL UAV — T Works - India's largest prototyping centre — Hyderabad*. en-GB. URL: https://tworks.telangana.gov.in/blog/tag/Hybrid+VTOL+UAV (visited on 03/24/2022).

[2] *YANGDA VTOL Drone For Long Range Package Delivery*. en-GB. URL: https://www.youtube.com/watch?v=-EuLftx49r8 (visited on 03/24/2022).

[3] *India's First Hybrid e-VTOL Drone delivery to transport life saving drugs in Meghalaya - TechEagle*. en-GB. URL: https://www.youtube.com/watch?v=kkNoHSr-zSk (visited on 03/24/2022).

[4] *Army Testing Drones for Medical Logistics*. en. URL: https://www.nationaldefensemagazine.org/articles/2022/1/7/army-testing-drones-for-medical-logistics (visited on 03/24/2022).

[5] Wikipedia. *First Geneva Convention — Wikipedia, The Free Encyclopedia*. http://en.wikipedia.org/w/index.php?title=First%20Geneva%20Convention&oldid=1075356436. [Online; accessed 24-March-2022]. 2022.

[6] Christopher K. Gilmore, Michael Chaykowsky, and Brent Thomas. *Autonomous Unmanned Aerial Vehicles for Blood Delivery: A UAV Fleet Design Tool and Case Study*. en. Tech. rep. RAND Corporation, Oct. 2019. URL: https://www.rand.org/pubs/research_reports/RR3047.html (visited on 03/24/2022).

[7] Target Information Systems Ltd. *JPAC - Transfusion Guidelines*. en. URL: https://transfusionguidelines.org.uk/ (visited on 03/24/2022).

[8] *Amazon.com: Military Individual First Aid Kit - IFAK : Health & Household*. URL: https://www.amazon.com/Military-Individual-First-Aid-Kit/dp/B07CVMXSVF (visited on 03/24/2022).

[9] *Sodium Chloride (Saline) 0.9 IV Bags 1000 mL (1-Bag)*. en. URL: https://www.mountainside-medical.com/products/sodium-chloride-0-9-saline-iv-bag-fluid-therapy (visited on 03/24/2022).

[10] *In the Air With Zipline's Medical Delivery Drones*. en. Apr. 2019. URL: https://spectrum.ieee.org/in-the-air-with-ziplines-medical-delivery-drones (visited on 03/24/2022).

[11] *Wing*. en. URL: https://wing.com/ (visited on 03/24/2022).

[12] Özgür Dündar, Mesut Bilici, and Tarık Ünler. "Design and performance analyses of a fixed wing battery VTOL UAV". In: *Engineering Science and Technology, an International Journal* 23.5 (2020), pp. 1182–1193. ISSN: 2215-0986. DOI: https://doi.org/10.1016/j.jestch.2020.02.002. URL: https://www.sciencedirect.com/science/article/pii/S2215098619316489.

[13] robu.in. *Orange 16000mAh 6S 25C/50C Lithium Polymer Battery Pack (LiPo)*. English. E-Commerce. publisher: www.robu.in. URL: https://robu.in/product/orange-16000mah-6s-25c50c-lithium-polymer-battery-pack-lipo/?gclid=CjwKCAiA4KaRBhBdEiwAZi1zziRE_FFNZFuSeZzrLqI5mpIG4Use2k7R0uS0sw4f2sUgUKyfPmthuBoC-5AQAvD_BwE.

[14] *Do low temperatures damage LiPo batteries?* en. URL: https://drones.stackexchange.com/questions/378/do-low-temperatures-damage-lipo-batteries (visited on 05/30/2022).

[15] Zhuomin Zhou, Xingzhen Zhou, Xiangsheng Zhou, Mao Li, Duankai Li, and Chen Deng. "Study on Thermal Insulation Material Selection for Lithium-Ion Power Battery System". In: *Proceedings of the 5th International Conference on Electrical Engineering and Information Technologies for Rail Transportation (EITRT) 2021*. Ed. by Yong Qin, Limin Jia, Jianying Liang, Zhigang Liu, Lijun Diao, and Min An. Singapore: Springer Singapore, 2022, pp. 110–116. ISBN: 978-981-16-9913-9.

[16] E. G. Tulapurkara. "Estimation of Wing Loading and Thrust Loading". English. In: *Aircraft Design (Aerodynamic)*. NPTEL Lectures on Aircraft Design (Aerodynamic). Indian Institute of Technology Madras, Chennai, India: NPTEL under Creative Commons License, Mar. 2022. URL: https://nptel.ac.in/courses/101106035 (visited on 03/31/2022).

[17] H. C. M. Veerman. "Preliminary multi-mission UAS design". en. In: (2012). URL: https://repository.tudelft.nl/islandora/object/uuid%3A6762136d-5f8c-46a8-9ee5-18347c43fc0e (visited on 05/30/2022).

[18] Ashraf M Kamal and Alex Ramirez-Serrano. "Design methodology for hybrid (VTOL+ Fixed Wing) unmanned aerial vehicles". In: *Aeronautics and Aerospace Open Access Journal* 2.3 (2018), pp. 165–176.

[19] Mohammad H Sadraey. *Aircraft design: A systems engineering approach*. John Wiley & Sons, 2012.

[20] *BigFoil*. URL: http://bigfoil.com/ (visited on 05/30/2022).

[21] Daniel Raymer. *Aircraft design: a conceptual approach*. American Institute of Aeronautics and Astronautics, Inc., 2012.

[22] Jan Roskam. *Airplane Design*. en. Google-Books-ID: GIHHFkd829cC. DARcorporation, 1985. ISBN: 9781884885556.